The Plant Cell, Vol. 24: 1675–1690, April 2012, www.plantcell.org

Requirement of the Cytosolic Interaction between PATHOGENESIS-RELATED PROTEIN10 and LEUCINE-RICH REPEAT PROTEIN1 for Cell Death and Defense Signaling in Pepper [W]

Du Seok Choi, In Sun Hwang,[1] and Byung Kook Hwang[2]

Laboratory of Molecular Plant Pathology, School of Life Sciences and Biotechnology, Korea University, Seoul 136-713, Republic of Korea

Plants recruit innate immune receptors such as leucine-rich repeat (LRR) proteins to recognize pathogen attack and activate defense genes. Here, we identified the pepper (*Capsicum annuum*) pathogenesis-related protein10 (PR10) as a leucine-rich repeat protein1 (LRR1)–interacting partner. Bimolecular fluorescence complementation and coimmunoprecipitation assays confirmed the specific interaction between LRR1 and PR10 in planta. Avirulent *Xanthomonas campestris* pv *vesicatoria* infection induces *PR10* expression associated with the hypersensitive cell death response. Transient expression of *PR10* triggers hypersensitive cell death in pepper and *Nicotiana benthamiana* leaves, which is amplified by *LRR1* coexpression as a positive regulator. LRR1 promotes the ribonuclease activity and phosphorylation of PR10, leading to enhanced cell death signaling. The LRR1-PR10 complex is formed in the cytoplasm, resulting in its secretion into the apoplastic space. Engineered nuclear confinement of both proteins revealed that the cytoplasmic localization of the PR10-LRR1 complex is essential for cell death–mediated defense signaling. *PR10/LRR1* silencing in pepper compromises resistance to avirulent *X. campestris* pv *vesicatoria* infection. By contrast, *PR10/LRR1* overexpression in *Arabidopsis thaliana* confers enhanced resistance to *Pseudomonas syringae* pv *tomato* and *Hyaloperonospora arabidopsidis*. Together, these results suggest that the cytosolic LRR-PR10 complex is responsible for cell death–mediated defense signaling.

INTRODUCTION

Plants have evolved resistance mechanisms to overcome microbial pathogen attack. Disease resistance (R) proteins mediate the recognition of pathogen invasion and elicit downstream signaling responses, leading to plant immunity (Moffett et al., 2002). Programmed cell death (PCD), often the ultimate endpoint of extreme defense, limits the spread of invasive pathogens. In the compatible plant–pathogen interactions, pathogens repress plant immunity using effectors that cause disease symptoms. However, plant recognition of these effectors triggers the hypersensitive response (HR) in the incompatible interactions. This is called effector-triggered immunity and is a stronger immune response than pathogen-associated molecular pattern–triggered immunity.

The leucine-rich repeat (LRR) domain is a conserved feature of many R proteins, including nucleotide binding (NB) and LRR proteins (Dangl and Jones, 2001). Plant NB-LRRs perceive their effector ligands using their N terminus (Gutierrez et al., 2010). LRR-containing receptor-like kinases (RLKs), including FLAGELLIN-SENSITIVE2 and EF-TU RECEPTOR, recognize bacterial flagellin and translational elongation factor EF-Tu, respectively (Gómez-Gómez and Boller, 2000; Zipfel et al., 2006). Another LRR-RLK, BRASSINOSTEROID INSENSITIVE1, perceives plant steroid hormone brassinosteroids (Wang et al., 2001). The pepper (*Capsicum annuum*) LRR1 contains a single LRR domain with five tandem repeats of a 24–amino acid LRR motif (Jung et al., 2004). LRR1, which is lacking a kinase domain, exhibits sequence similarity to RLKs and has been implicated in the plant defense response (Jung et al., 2004; Jung and Hwang, 2007). LRR1 interacts with the pepper HYPERSENSITIVE-INDUCED REACTION PROTEIN1 (HIR1) that triggers HR during avirulent *Xanthomonas campestris* pv *vesicatoria* (*Xcv*) infection. This ultimately leads to compromised HIR1-induced HR (Jung and Hwang, 2007). More recently, LRR1 and HIR1 have been demonstrated to act as cell death regulators associated with plant immunity and disease, respectively (Choi et al., 2011).

Convincing evidence indicates that the pathogenesis-related10 (PR10) family, one of the pathogenesis-related groups, has distinct functions in developmental processes, secondary metabolism, and antimicrobial activity (McGee et al., 2001; Zhou et al., 2002; Hashimoto et al., 2004; Park et al., 2004; Liu and Ekramoddoullah, 2006). Sequence analysis of the PR10 family indicates similarity with a major birch (*Betula alba*) pollen allergen Bet v 1 (Breiteneder et al., 1989). More recently, a positive transcription factor, *WRKYb*, was demonstrated to bind the *PR10* promoter and activate the defense signaling pathway in pepper (Lim et al., 2011). Several

[1] Current address: Boyce Thompson Institute for Plant Research, Tower Road, Ithaca, NY 14853-1801.
[2] Address correspondence to bkhwang@korea.ac.kr.
The author responsible for distribution of materials integral to the findings presented in this article in accordance with the policy described in the Instructions for Authors (www.plantcell.org) is: Byung Kook Hwang (bkhwang@korea.ac.kr).
[W] Online version contains Web-only data.
www.plantcell.org/cgi/doi/10.1105/tpc.112.095869

PR10 family genes were isolated from various plant species, including apple (*Malus domestica*), asparagus (*Asparagus officinalis*), parsley (*Petroselinum crispum*), bean (*Phaseolus vulgaris*), pea (*Pisum sativum*), sorghum (*Sorghum bicolor*), potato (*Solanum tuberosum*), pepper, and rice (*Oryza sativa*) (Somssich et al., 1986; Matton and Brisson, 1989; Walter et al., 1990; Warner et al., 1992; Lo et al., 1999; Pühringer et al., 2000; Park et al., 2004; Hashimoto et al., 2004). The *PR10* genes are induced by microbial attack (Somssich et al., 1986), fungal elicitors (Somssich et al., 1986; Walter et al., 1990), or wounding stress (Warner et al., 1992). In general, *PR10* genes are specifically induced in response to abiotic and biotic stress. However, the specific functions of PR10 in plant immunity and cell death signaling remain to be clarified.

Cell death localized at the infection site is the strongest strategy to restrict pathogen growth and development. This cell death response often includes the induction of *R* gene expression, ion fluxes, and the accumulation of reactive oxygen species (ROS) and defense-related hormones, such as salicylic acid (SA) (Li et al., 2010; Melech-Bonfil and Sessa, 2010). The constitutive activation of defense by genetic modification leads to spontaneous HR-like cell death lesions in the absence of pathogens (Lorrain et al., 2003). These so-called lesion mimic mutants often exhibit dwarf-like phenotypes due to constitutive defense activation (Dangl et al., 1996; Mosher et al., 2010). For example, rice *blast lesion mimic* mutants, which show a spontaneous cell death phenotype, significantly induce high levels of PR10s (Os-PR10a and Os-PR10b) (Jung et al., 2005, 2006).

Some plant resistance proteins have been convincingly demonstrated to localize and act in specific cellular compartments to trigger innate immunity signaling. *Arabidopsis thaliana* Toll/Interleukin-1–type NB-LRR receptor RESISTANCE TO PSEUDOMONAS SYRINGAE4 (RPS4) accumulates in the nucleus to trigger *ENHANCED DISEASE SUSCEPTIBILITY1*–dependent defense signaling (Gassmann et al., 1999; Wirthmueller et al., 2007). Tobacco (*Nicotiana tabacum*) N protein, which confers resistance against *Tobacco mosaic virus*, functions in the nucleus to trigger complex downstream defense events (Burch-Smith et al., 2007). In a previous study, the nuclear localization of pepper ABSCISIC ACID-RESPONSIVE1 (ABR1) was shown to be essential as a hypersensitive cell death regulator, despite the lack of a discernible nuclear localization signal (NLS) in ABR1 (Choi and Hwang, 2011). By contrast, some R proteins act in the cytoplasm. Potato NB-LRR receptor RX1, which confers a high resistance to *Potato virus X*, is located in both the cytoplasm and the nucleus (Slootweg et al., 2010). However, Rx1 is activated in the cytoplasm but not in the nucleus. The other NB-LRR protein, RPM1 (for Resistance to *Pseudomonas syringae* pv *maculicola1*), is activated at and functions on the plasma membrane (Gao et al., 2011).

Here, we report the identification of the pepper PR10 as a pepper LRR1-interacting partner using a yeast two-hybrid screen. Bimolecular fluorescence complementation (BiFC) and coimmunoprecipitation (co-IP) assays revealed that the intracellular protein PR10 specifically interacts with LRR1 in planta. *Agrobacterium tumefaciens*–mediated transient coexpression of *PR10* and *LRR1* prompted *PR10*-triggered hypersensitive cell death in pepper and *Nicotiana benthamiana* leaves. Upon fusing a nonfunctional NLS sequence (nls) to LRR1 and PR10, the cytoplasmic localization of these proteins was shown to be essential for cell death induction. Virus-induced gene silencing (VIGS) of *PR10* in pepper compromised the resistance responses against avirulent *Xcv* infection. By contrast, heterologous *PR10* overexpression in *Arabidopsis* conferred enhanced resistance to *Pseudomonas syringae* pv *tomato* and *Hyaloperonospora arabidopsidis* infection. Taken together, these results demonstrate that cytoplasmic PR10 functions in HR-like cell death and defense signaling. Furthermore, this role is strengthened by interaction with LRR1.

RESULTS

Expression of *LRR1* and *PR10* in Pepper

RNA and immunoblot analyses were used to characterize further the differential transcriptional and posttranscriptional patterns of *PR10* expression in pepper plants (see Supplemental Figure 1 online). Infection with avirulent (incompatible) *Xcv* strain Bv5-4a triggered the strong and early induction of *PR10* in pepper leaves. Although infection with the virulent (compatible) strain Ds1 resulted in strong transcriptional expression of *PR10* (see Supplemental Figure 1A online), immunoblot analysis using PR10-specific antibody revealed that the PR10 induction was specific to the pepper leaves infected with the avirulent (incompatible) *Xcv* strain Bv5-4a (see Supplemental Figure 1B online). Infection with avirulent *Xcv* strain Bv5-4a caused a rapid induction of the hypersensitive cell death response (HR) in pepper leaves within 24 h of infiltration with a high titer (10^8 colony-forming units [cfu] mL^{-1}).

PR10 Interacts with LRR1

The pepper *LRR1* gene was previously isolated from pepper leaves infected with *Xcv* (Jung et al., 2004). To isolate defense-related proteins in pepper, a pepper cDNA library generated from avirulent *Xcv*-infected leaves was screened for LRR1-interacting proteins using a GAL4-based yeast two-hybrid system. Among the clones identified from the screening, pepper PR10 was selected for further characterization as an interacting partner of LRR1 (Figure 1A).

The LRR1-PR10 interaction in planta was examined using a BiFC assay (Walter et al., 2004). N- and C-terminal portions of yellow fluorescent protein (YFP) were fused to LRR1 and PR10 to yield LRR1-YFP^N and PR10-YFP^C, respectively. The reciprocal constructs were also generated (LRR1-YFP^C and PR10-YFP^N). Interactions between the fusion proteins were visualized in *N. benthamiana* leaves following *Agrobacterium*-mediated transient expression. Confocal images of BiFC signals were detected in the cytoplasmic region (Figure 1B), indicating that PR10 binds to LRR1 in the cytoplasm of plant cells. The nuclear localization of bZIP63-YFP fusion proteins was used as a positive control.

Additionally, the LRR1 and PR10 interaction in planta was confirmed by co-IP using a transient coexpression system in *N. benthamiana* (Figure 1C). Proteins extracted from transiently expressing *N. benthamiana* leaves were incubated with α-hemagglutinin (HA) antibody to immunoprecipitate LRR1. Potential LRR1 and PR10 complexes were separated by SDS-PAGE. Immunoblotting using α-Myc antibody detected PR10.The co-IP

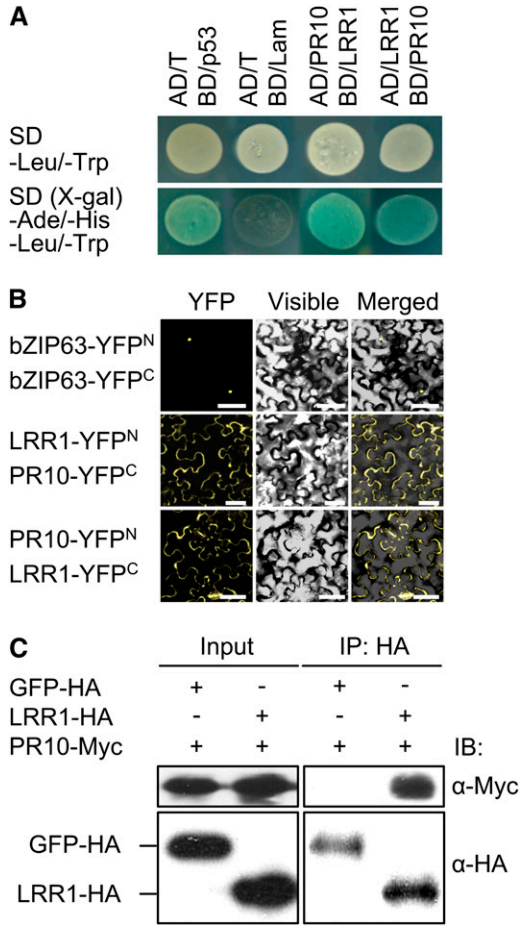

Figure 1. Interaction between LRR1 and PR10 in Yeast and *N. benthamiana.*

(A) LRR1 interacts with PR10 in a GAL4-based yeast two-hybrid system. SD, synthetic dropout. The plasmids encoding the fusions to the GAL4 AD and the DNA BD are denoted by AD and BD, respectively. Combinations of the Simian Vacuolating Virus 40 large T antigen (AD/T) with the murine p53 (BD/p53) fusion constructs and human lamic C (BD/Lam) were included as positive and negative controls, respectively.
(B) BiFC visualization of the LRR10/PR10 interaction in leaves infiltrated with *Agrobacterium*. Yellow fluorescence, visible light, and merged images were taken from the epidermal cells. The *bZIP63*-YFP^N and *bZIP63*-YFP^C constructs were used as positive controls. Bars = 50 μm.
(C) Co-IP and immunoblotting (IB) of GFP-HA or LRR1-HA and PR10-Myc proteins coexpressed in leaves. GFP-HA was used as a negative control.

assay revealed that PR10 physically interacts with LRR. By contrast, green fluorescent protein (GFP), included as a negative control, did not exhibit any interaction.

Transient Coexpression of *LRR1* and *PR10* Induces Cell Death and Defense Responses

An *Agrobacterium*-mediated transient expression assay was used to determine the effect of *LRR1* and *PR10* expression on the induction of the cell death response in pepper leaves (Figure 2).

The simultaneous expression of both LRR1 and PR10 in the agroinfiltrated leaves was confirmed using immunoblot analysis (Figure 2A). PR10 was more rapidly and more strongly expressed than LRR1. Plants transiently expressing the empty vector or *LRR1* did not trigger any cell death response in pepper leaves

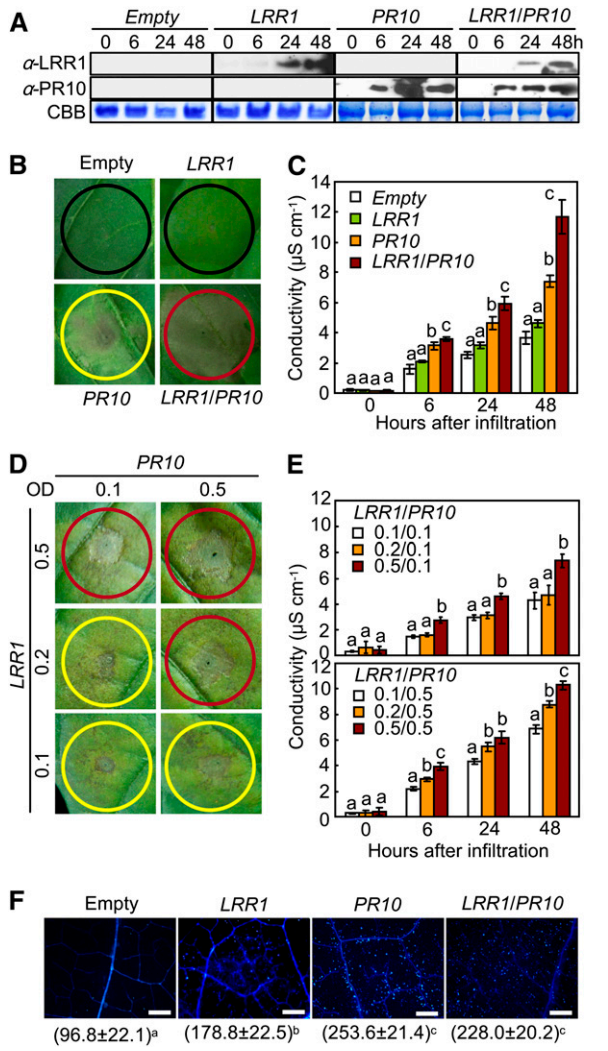

Figure 2. Transient Expression of *LRR1*, *PR10*, and *LRR1/PR10* in Pepper Leaves.

(A) Immunoblot analysis of the transient expression of LRR1, PR10, and LRR1/PR10. CBB, Coomassie blue staining of the gel to show equal loading.
(B) and **(C)** Cell death phenotypes **(B)** and electrolyte leakage **(C)** in leaves infiltrated with *Agrobacterium* strain GV3101 carrying 35S:00 (empty), 35S:*LRR1*, 35S:*PR10*, or 35S:*LRR1*/35S:*PR10*. Red, yellow, and black circles indicate full, partial, and no cell death, respectively.
(D) and **(E)** Cell death phenotypes **(D)** and electrolyte leakage **(E)** in leaves infiltrated with *Agrobacterium* at different inoculum ratios.
(F) Callose deposition (bright blue dots) in leaves infiltrated with *Agrobacterium*. Number of callose deposits mm^{-2} represents the mean ± SD from three leaf discs. Bars = 500 μm.
(C), **(E)**, and **(F)** Data represent the means ± SD from three independent experiments. Different letters above the bars indicate significantly different means ($P < 0.05$), as analyzed by Fisher's protected LSD test.

(Figure 2B). By contrast, *PR10* transient expression induced partial necrotic cell death. However, transient coexpression of *LRR1* and *PR10* was much more effective in triggering the full hypersensitive cell death response than was transient expression of *PR10* alone (Figure 2B). The synergistic effect of LRR1 as a positive regulator of cell death induction by *PR10* transient expression was supported by electrolyte leakage data (Figure 2C). Transient coexpression of *LRR1* and *PR10* resulted in enhanced electrolyte leakage from the pepper leaves, the magnitude of which was greater than that caused by the transient expression of *PR10* alone. Infiltration with greater concentrations of *Agrobacterium* carrying *LRR1* resulted in enhanced cell death induction by *PR10* transient expression in pepper leaves (Figure 2D). Transient coexpression of *LRR1*/*PR10* by infiltration with higher inoculum ratios of *Agrobacterium* carrying *LRR1* stimulated higher electron leakage from pepper leaf tissues (Figure 2E). The leaves infiltrated with *Agrobacterium* carrying either *PR10* or *LRR1*/*PR10* exhibited significantly higher levels of cell death–associated callose deposition than did the leaves infiltrated with *Agrobacterium* carrying either the empty vector or *LRR1* (Figure 2F).

To compare the cell death induction by *LRR1*/*PR10* coexpression with that induced by *Bcl2-ASSOCIATED X PROTEIN* (*BAX*) or *avrPto*/*Pto* expression, *Bax* and *avrPto*/*Pto* were used as positive inducers of cell death in *N. benthamiana* leaves (Figure 3). Mammalian Bax is capable of inducing cell death in plants (Lacomme and Santa Cruz, 1999), and the AvrPto interaction with Pto triggers HR in effector-triggered immunity (Tang et al., 1996). In contrast with the results of the pepper transient expression assay, neither *LRR1* nor *PR10* transient expression was able to trigger the cell death response in *N. benthamiana* leaves, despite agroinfiltration with an inoculum greater than OD_{600} = 1.0 (Figure 3A). However, coexpression of *LRR1* and *PR10* induced a cell death response similar to that triggered by *Bax* or *avrPto*/*Pto* expression. A quantitative analysis using an ion conductivity assay confirmed the cell death induction by *LRR1*/*PR10* transient coexpression (Figure 3B). Electrolyte leakage from leaves transiently expressing *LRR1*/*PR10* was significantly higher than from leaves transformed with empty vector, *LRR1* or *PR10*. However, electrolyte leakage due to *LRR1*/*PR10* expression was somewhat less than the levels induced by *Bax* or *avrPto*/*Pto* expression. Real-time RT-PCR analysis revealed an increase in the expression of *LRR1* and *PR10* 24 h after agroinfiltration (Figure 3C). The coexpression effects of *LRR1* and *PR10* on the cell death response in leaves were assessed by monitoring the well-known cell death marker genes *HYPERSENSITIVE-RELATED203J* (*HSR203J*) (Pontier et al., 1994) and *VACUOLAR PROCESSING ENZYME1a* (*VPE1a*) (Zhang et al., 2010). In leaves coexpressing *LRR1* and *PR10*, *HSR203J* induction was significantly greater than that observed following the transient expression of *LRR1* or *PR10*, though slightly lower than those observed following *avrPto* or *Bax* expression (Figure 3C). *VPE1a*, involved in elicitor-triggered immunity in *N. benthamiana* (Zhang et al., 2010), was also significantly induced by *LRR1* and *PR10* coexpression (Figure 3C). However, transient expression of *LRR1* or *PR10* individually did not trigger *HSR203J* or *VPE1a* expression in *N. benthamiana* leaves (Figure 3C).

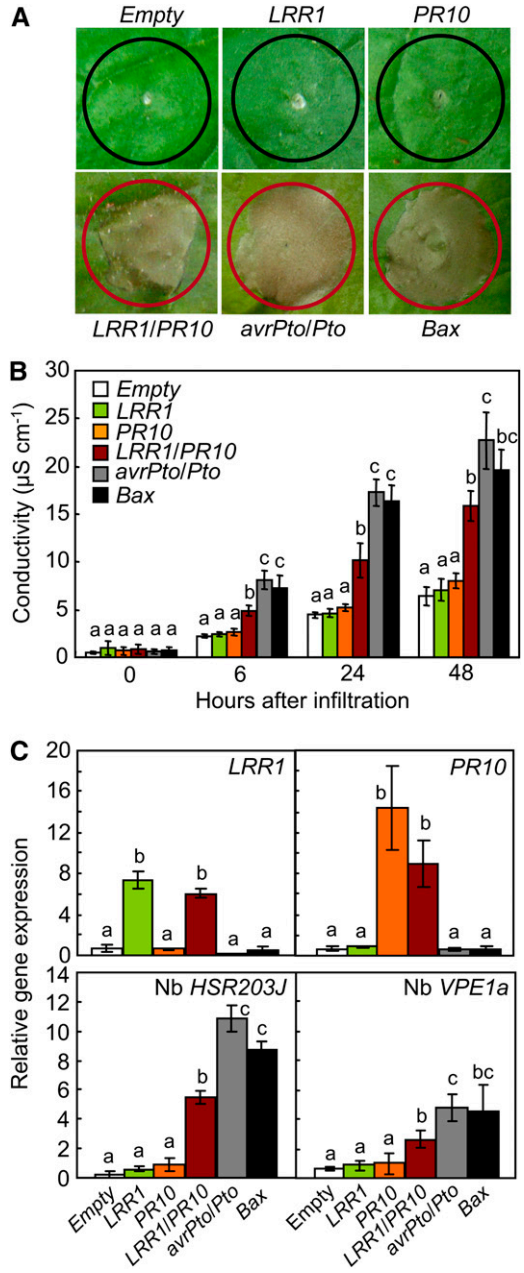

Figure 3. Transient Expression of LRR1, PR10, LRR1/PR10, avrPto/Pto, and Bax in *N. benthamiana* Leaves.

(A) Cell death phenotypes in leaves infiltrated with *Agrobacterium* strain GV3101 carrying different constructs. Red and black circles indicate full and no cell death, respectively.

(B) Quantification of electrolyte leakage as ion conductivity to assess the cell death response in leaf discs.

(C) Quantitative real-time RT-PCR analysis of the expression of *LRR1*, *PR10*, *HSR203J*, and *VPR1a* in *N. benthamiana* leaves 24 h after agroinfiltration.

(B) and **(C)** Data represent the means ± SD from three independent experiments. Different letters above the bars indicate significantly different means ($P < 0.05$), as analyzed by Fisher's protected LSD test.

LRR1 Promotes the Ribonuclease Activity and Phosphorylation of PR10

In-gel RNase assay (Bufe et al., 1996) was used to investigate whether LRR1 affects the RNase activity of PR10. The recombinant PR10, but not LRR1, distinctly degraded torula yeast (*Candida utiliz*) RNA (Figure 4A), indicating that PR10 possesses RNase activity. For the RNA degradation assay, the recombinant proteins (LRR1, PR10, and LRR1/PR10) and elution buffer were incubated with torula yeast RNA. As shown in Figure 4B, recombinant LRR1 with no RNase activity significantly enhanced PR10-mediated RNA degradation in a dose-dependent manner.

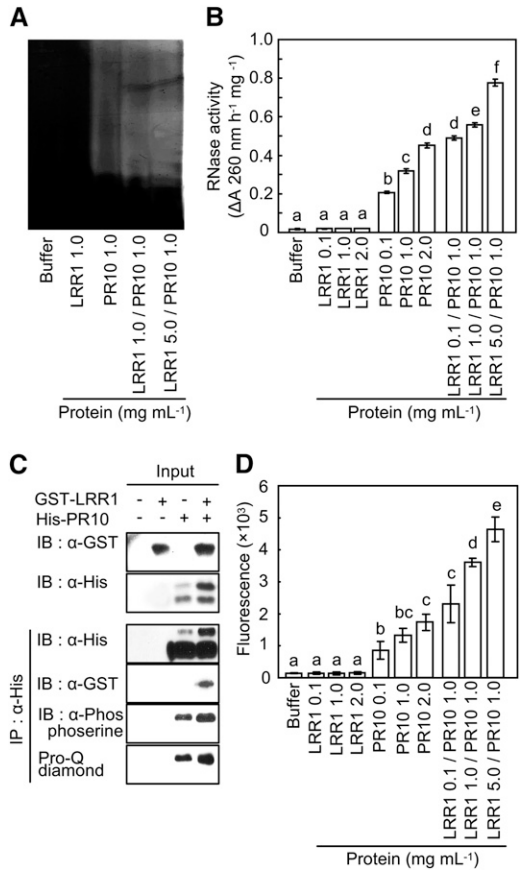

Figure 4. Synergistic Effect of LRR1 on RNase Activity and Phosphorylation of PR10.

(A) Detection of RNase activity of PR10 on 15% acrylamide gel containing yeast RNA. After electrophoresis of recombinant PR10 and LRR1 proteins mixed at different concentrations, the gel was stained with toluidine blue O.

(B) RNase activity assay of PR10 in the presence of LRR1 using yeast RNA.

(C) Pro-Q diamond staining and immunoblot (IB) analysis using a phosphoserine antibody for the detection of PR10 phosphorylation.

(D) Quantification of phosphorylation by the detection of Pro-Q diamond fluorescence using ProXPRESS. Phosphorylation reactions were done using different concentrations of PR10 and LRR1 (0.1 to ~5.0 μg).

(B) and **(D)** Data represent the means ± SD from three independent experiments. Different letters indicate significantly different means, as analyzed by Fisher's protected LSD test ($P < 0.05$).

To phosphorylate PR10 by certain protein kinases, we used crude protein extracts from pepper leaves infected with avirulent *Xcv* Bv5-4a. The phosphorylated PR10 was detectable by Pro-Q diamond gel staining (Figure 4C). Immunoblot analysis using the antiphosphoserine antibody confirmed the phosphorylation of PR10 by protein extracts of pepper leaves (Figure 4C). In parallel, immunoblot analysis using anti-His and anti-glutathione *S*-transferase (GST) antibodies detected recombinant PR10 and LRR1 in the phosphorylation reactions, respectively. As expected, increases in the amount of LRR1 added to the reactions significantly enhanced the PR10 phosphorylation. Quantification of the Pro-Q diamond staining data by fluorescence measurements revealed that PR10 bound to LRR1 resulted in significantly higher levels of phosphorylation than did PR10 alone (Figure 4D). Collectively, these results indicate that LRR1 positively regulates the phosphorylation and RNase activity of PR10.

Cytoplasmic Localization of the LRR1-PR10 Complex Is Essential for Cell Death Induction

The subcellular locations of GFP-fused LRR1 and PR10 in *N. benthamiana* leaves were visualized using a confocal microscope. Both proteins were detected in the cytoplasm but not in the nuclei (Figure 5A). To determine the localization sites of LRR1 and PR10 in planta, a time course of BiFC assay signals was analyzed (see Supplemental Figure 2 online). Yellow fluorescent LRR1-PR10 complexes were detected in the cytoplasm 24 h after agroinfiltration. At 48 h after agroinfiltration, the LRR1-PR10 complex initiated an efflux into the extracellular region. To examine whether the protein complex moves from the cytoplasm to the extracellular regions, *N. benthamiana* leaves were infiltrated with brefeldin A (BFA), an inhibitor of secretion (Staehelin and Driouich, 1997), following the coexpression of *LRR1* and *PR10*. In this localization experiment, BFA treatment resulted in the aggregation of YFP within the cells (see Supplemental Figure 3 online). By contrast, the BiFC signals of the LRR1-PR10 interaction were observed in the cytoplasm and the extracellular space in the absence of BFA. These results indicate that the LRR1-PR10 complex may interact in the cytoplasm to cause secretion into the apoplast via the plasma membrane. Varients of LRR1 and PR10 that would localize to the nucleus were generated by fusion with a well-known Simian Vacuolating Virus 40 NLS (PKKKRKV) (Hodel et al., 2001; Slootweg et al., 2010). Confocal microscopy images demonstrated that the NLS fusion was sufficient to target the NLS-LRR1-GFP or NLS-PR10-GFP proteins to the nuclei (Figure 5A). The nonfunctional NLS mutant (nls) was used to express nls-fused PR10 and LRR1 in the cytoplasm. The NLS or nls fusion proteins were further introduced into the BiFC vectors, pSPYNE and pSPYCE, to investigate which location of the LRR1-PR10 complex is essential for cell death induction. Transient coexpression of NLS-LRR1-YFP^N and NLS-PR10-YFP^C was detected as yellow fluorescence signals in the nuclei (Figure 5B). This indicates that both fusion proteins localized to the nuclei and interact with each other. Similarly, coexpression of nls-LRR1-YFP^N and nls-PR10-YFP^C produced BiFC signals in the cytoplasm, indicating a physical interaction between both proteins. However, no yellow fluorescence signals

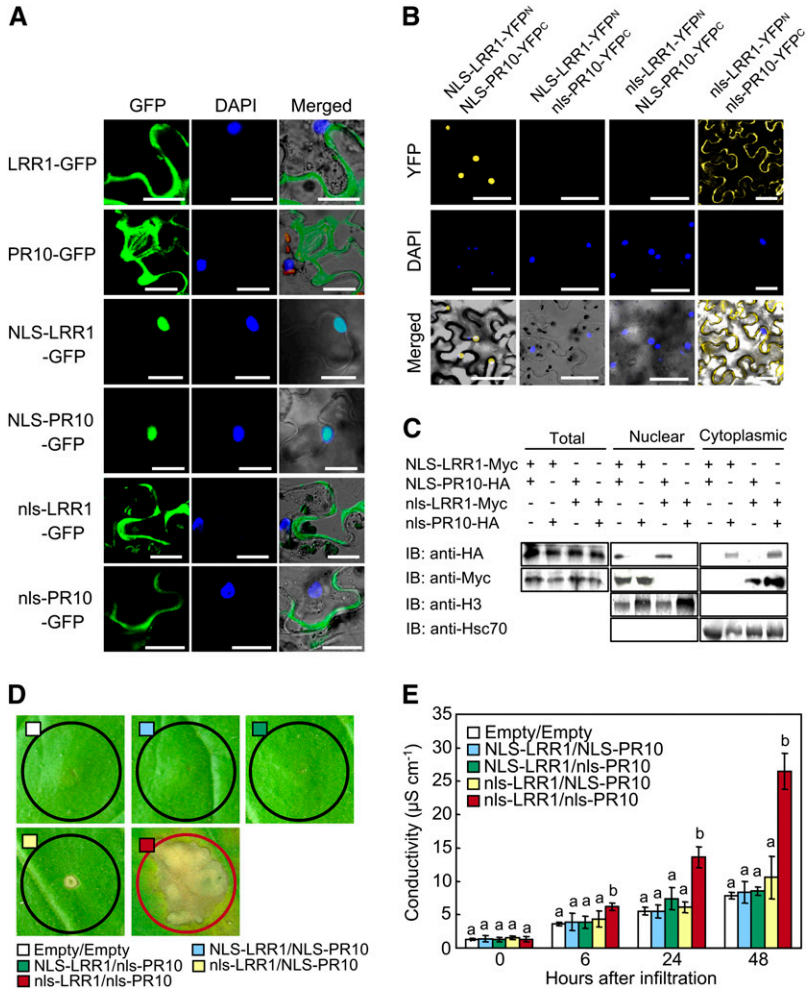

Figure 5. Cytoplasmic Localization of the LRR1/PR10 Complex Is Essential for Cell Death Induction.

(A) Subcellular localization of NLS- or nls-fused LRR1 and PR10 in *N. benthamiana* leaves. DAPI images indicate nuclear staining. All images were taken by confocal microscopy 24 h after agroinfiltration. Bars = 20 μm.

(B) BiFC images of NLS- or nls-fused LRR10/PR10 combinations in leaves infiltrated with *Agrobacterium*. Bars = 50 μm.

(C) Immunoblot (IB) analysis of LRR1-Myc and PR10-HA in nuclear and cytoplasmic fractions of leaves transiently expressing NLS- or nls-fused LRR1 or PR10. Histone H3 and Hsc70 were included as fractionation markers for the nucleus and the cytoplasm, respectively.

(D) Induction of the cell death response by transient expression of nls-fused LRR10/PR10 combinations 3 d after agroinfiltration.

(E) Quantification of electrolyte leakage as ion conductivity to assess the cell death response. Data represent the means ± SD from three independent experiments. Different letters indicate significantly different means, as analyzed by Fisher's protected LSD test ($P < 0.05$).

were detected in *N. benthamiana* leaf cells upon the coexpression of NLS-fused LRR1 and nls-fused PR10, and vice versa. When analyzed by immunoblotting, NLS-fused LRR1 or PR10 proteins were detected in the nuclear fractions. However, nls-fused proteins were observed in the nucleus-depleted fractions (Figure 5C). Histone 3 (H3) and heat shock complex 70 were detected in the nuclear and cytoplasmic fractions, respectively (Figure 5C).

Nuclear or nucleocytoplasmic coexpression of NLS- or nls-fused LRR1 and PR10 did not trigger the cell death response in *N. benthamiana* leaves (Figure 5D). By contrast, the coexpression of nls-LRR1 and nls-PR10 induced the hypersensitive cell death response 3 d after agroinfiltration and also significantly increased electrolyte leakage from *N. benthamiana* leaves (Figure 5E). Together, these results suggest that the cytoplasmic coexpression of the LRR1-PR10 complex is required for cell death induction in *N. benthamiana* leaves.

Silencing of *PR10* Attenuates Disease Resistance and Compromises the Hypersensitive Cell Death Response

To study the loss of function of *PR10* and/or *LRR1*, we generated *LRR1*- and/or *PR10*-silenced pepper plants using the VIGS technique. Quantitative real-time RT-PCR analysis showed that *LRR1*, *PR10*, or *LRR1/PR10* was effectively silenced in plants infected with *Xcv* (see Supplemental Figure 4 online). Avirulent *Xcv* growth in *PR10*- or *LRR1/PR10*-silenced leaves increased to significantly

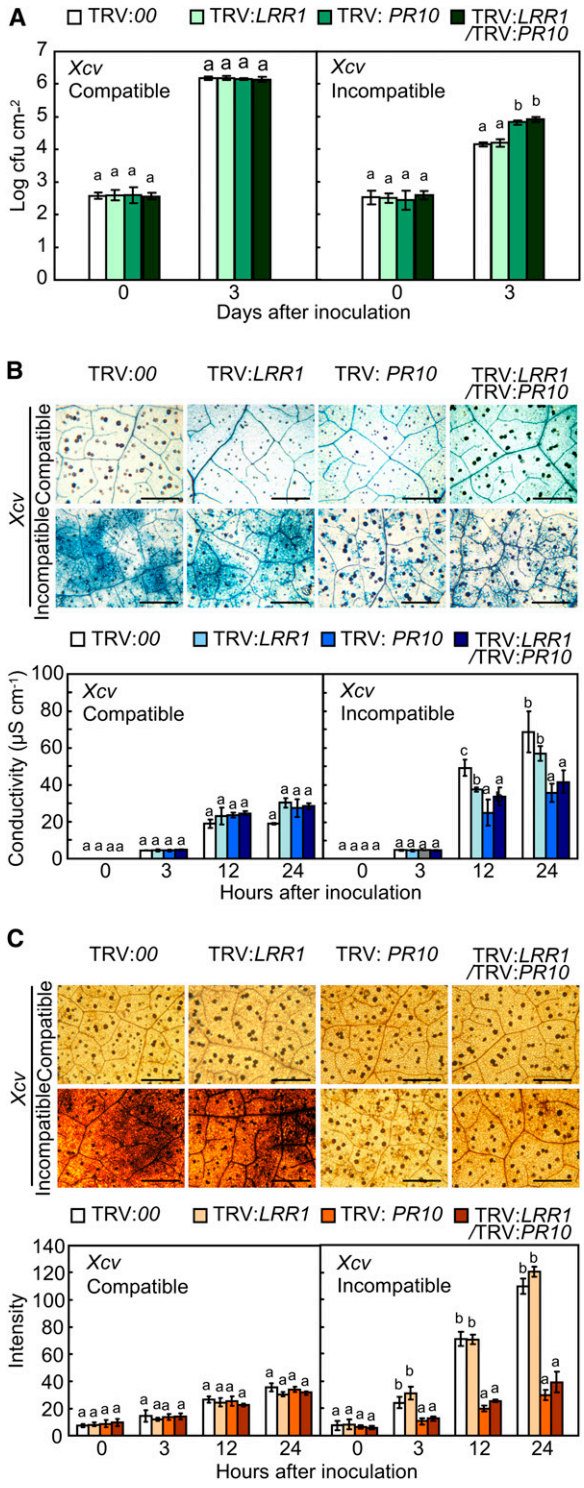

Figure 6. Distinct Responses of *LRR1*-, *PR10*-, and *LRR1/PR10*-Silenced Pepper Plants to *Xcv* Infection.

(A) Bacterial growth in leaves infected with *Xcv* (5×10^4 cfu mL^{-1}).

(B) Trypan blue staining (top) with leaves 24 h after inoculation with *Xcv* (10^7 cfu mL^{-1}). Quantification of electrolyte leakage (bottom) from leaves infected with *Xcv* (10^7 cfu mL^{-1}). Bars = 500 μm.

(C) DAB staining (top) to detect H_2O_2 production in leaves infected with *Xcv* (10^7 cfu mL^{-1}). Quantification of H_2O_2 production in leaf tissues (bottom), as determined by ImageJ software. Bars = 500 μm.

Data represent the means ± SD from three independent experiments. Different letters indicate significant differences, as determined by Fisher's protected LSD test ($P < 0.05$).

higher levels than that in the empty vector controls (Figure 6A). However, the silencing of *LRR1* did not enhance avirulent bacterial growth. Notably, the silencing of both genes did not affect the proliferation of *Xcv* virulent (compatible) Ds1 in pepper leaves. Trypan blue staining of leaves demonstrated that *PR10* silencing compromises the HR in the incompatible interaction (Figure 6B, top panel). The visual scores of the cell death phenotype were substantiated by an electrolyte leakage assay (Figure 6B, bottom panel). Inhibition of electrolyte leakage from *PR10*- or *LRR1/PR10*-silenced leaves was significantly greater than that in unsilenced or *LRR1*-silenced leaves during the avirulent *Xcv* infection. The trypan blue staining and ion conductivity data further indicate that *PR10*, but not *LRR1*, triggers pathogen-induced hypersensitive cell death response in pepper. To determine if the silencing of *LRR1* and *PR10* inhibits ROS accumulation, *Xcv*-infected leaves were stained with 3,3′-diaminobenzidine tetrahydrochloride (DAB), a histochemical reagent for hydrogen peroxide (H_2O_2). As expected, *PR10*- and *LRR1/PR10*-silenced leaves also accumulated significantly lower levels of H_2O_2 than the unsilenced and *LRR1*-silenced leaves at the early stage of *Xcv* infection (Figure 6C).

Quantitative RT-PCR analysis was used to investigate whether *LRR1* and *PR10* silencing regulates defense response genes in pepper leaves during *Xcv* infection (Figure 7A). *PATHOGENESIS-RELATED PROTEIN1* (*PR1*; Kim and Hwang, 2000), *Defensin1* (*DEF1*; Do et al., 2004), *SYSTEMIC ACQUIRED RESISTANCE8.2* (*SAR82*; Lee and Hwang, 2003), and *PEROXIDASE2* (*PO2*; Choi et al., 2007) were significantly downregulated in pepper leaves that had been silenced for *LRR1/PR10* during *Xcv* infection, especially in the incompatible interactions (Figure 7A). Silencing of *LRR1*, *PR10*, or *LRR1/PR10* did not significantly compromise the induction of free and total SA by the *Xcv* virulent (compatible) infection (Figure 7B). By contrast, the accumulated free and total SA levels were significantly lower in all *LRR1*- and/or *PR10*-silenced leaves in comparison to the empty vector control leaves 24 h after inoculation with the *Xcv* avirulent (incompatible) Bv5-4a strain (Figure 7B). Notably, the silencing of *PR10* or *LRR1/PR10* distinctly suppressed the accumulation of SA and its glycoside (SAG) when compared with *LRR1* silencing in pepper leaves during the *Xcv* virulent (compatible) infection. Together, these results indicate that *PR10* is required for the hypersensitive cell death and defense responses, including HR induction, ROS burst, defense-related gene induction, and SA accumulation.

Enhanced Resistance of *PR10*- and *LRR1/PR10*-Overexpressing Transgenic *Arabidopsis* to Bacterial and Oomycete Infection

Resistance to *P. syringae* pv *tomato* (*Pst*) infection was investigated using *Arabidopsis* plants co-overexpressing *LRR1*, *PR10*, and *LRR1/PR10* (Figure 8). Notably, *PR10* overexpression (OX)

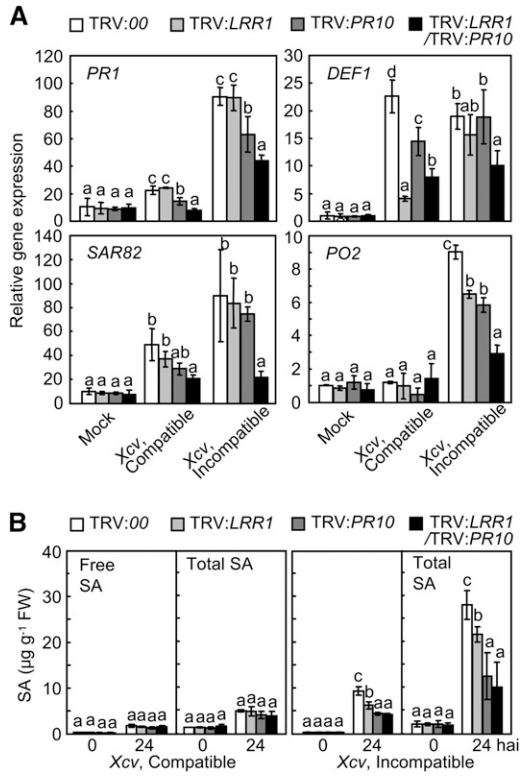

Figure 7. Silencing of *LRR1*/*PR10* Compromises Defense Gene Expression and SA Accumulation in Pepper Leaves Infected by *Xcv*.

(A) Quantitative real-time RT-PCR analysis of the expression of defense response genes in the leaves 24 h after *Xcv* inoculation. Expression values are normalized by the expression level of *Ca ACTIN*.

(B) Levels of free SA and total SA (free SA plus its conjugate) in the leaves infected by *Xcv*. FW, fresh weight.

Data represent the means ± SD from three independent experiments. Different letters indicate significant differences, as statistically analyzed by Fisher's protected LSD test ($P < 0.05$).

reduced chlorotic or necrotic disease symptoms in *Arabidopsis* leaves infected with *Pst* DC*3000* or DC*3000* (*avrRpm1*) (Figure 8A). Bacterial growth in the leaves of wild-type plants was similar to that in *LRR1*-OX plants. By contrast, *PR10* and *LRR1*/*PR10*-OX plants exhibited significantly less growth of *Pst* DC3000 and DC3000 (*avrRpm1*) than did wild-type and *LRR1*-OX plants (Figure 8B). Trypan blue–stained micrographs show that cell death induction by *Pst* infection was significantly accelerated in *PR10*- and *LRR1*/*PR10*-OX plants (Figure 8C). *Pst*-infected leaves were next stained with DAB, and the brownish color intensity was quantified using ImageJ. As expected, infection with *Pst* DC3000 and DC3000 (*avrRpm1*) drastically increased H_2O_2 accumulation in the leaves of *PR10*- and *LRR1*/*PR10*-OX plants in comparison to wild-type and *LRR1-OX* plants (Figure 8D). These data suggest that *LRR1* positively regulates cell death and the ROS burst caused by *PR10* overexpression. The representative defense marker gene *PR1* was significantly induced in *PR10*- and *LRR1*/*PR10*-OX *Arabidopsis* leaves infected by *Pst* DC3000, particularly in the interaction with *Pst* DC3000 (*avrRpm1*) (Figure 9). Expression of *SENESCENCE-ASSOCIATED GENE13* (*SAG13*), a gene encoding a short-chain alcohol dehydrogenase, is known to be required for PCD (Brodersen et al., 2002). The *SAG13* transcript levels in *PR10*- and *LRR1*/*PR10*-OX *Arabidopsis* leaves were significantly greater than those in wild-type Columbia-0 (Col-0) and *LRR1*-OX leaves during *Pst* DC3000 infection (Figure 9). NADPH oxidase *RESPIRATORY BURST OXIDASE HOMOLOG D* (*RbohD*) was not constitutively induced in any of the transgenic plants. However, *RbohD* expression was drastically heightened in *PR10*- and *LRR1*/*PR10*-OX leaves following *Pst* infection (Figure 9). Details of growth phenotypes and enhanced resistance of *PR10* transgenic *Arabidopsis* to *Pst* and *H. arabidopsidis* infection are shown in Supplemental Data Set 1 and Supplemental Figures 5 to 7 online.

Wild-type *Arabidopsis* (Col-0) cotyledons displayed a high level of mycelial growth, sporulation, and sporangiophore formation of the oomycete pathogen *H. arabidopsidis* isolate Noco2 (Figure 10; see Supplemental Figure 8 online). By contrast, transgenic expression of *LRR1*, *PR10*, and *LRR1*/*PR10* significantly decreased the growth and development of *H. arabidopsidis*, ultimately resulting in reduced disease development. Overexpression of these transgenes also conferred enhanced H_2O_2 production and callose accumulation around the infection sites, preventing further hyphal development (Figures 10A and 10B). Reduced sporulation and conidiopspore production was distinctly noticeable in the *PR10*- and *LRR1*/*PR10*-OX transgenic plants (Figures 10C and 10D). Notably, the double OX transgenic plants of *LRR1* and *PR10* were more resistant to this oomycete pathogen than were the wild-type and other single OX mutant plants.

DISCUSSION

In this article, we demonstrate that the pepper pathogenesis-related protein PR10, a member of the Bet v 1 allergen family, is crucial for defense and cell death responses against bacterial pathogen attack. To date, little is known concerning the cellular functions of PR10, although it is known to have ribonuclease and antimicrobial activity (Zhou et al., 2002; Park et al., 2004). In previous proteomics work, PR10 was isolated from pepper leaves infected with an avirulent *Xcv* strain (Choi and Hwang, 2011). As demonstrated with RNA gel blot and immunoblot analyses, *PR10* is strongly induced by avirulent *Xcv* infection. The convincing data prompted an investigation into the role of PR10 in the hypersensitive cell death and defense responses in plants.

PR10 Interacts with LRR1 to Activate Cell Death and Defense Responses

Up until now, there has been no experimental evidence indicating physical interaction between PR10 and other plant proteins. In this study, we found physical and functional interactions between the PR10 and LRR1 proteins to activate cell death and defense responses in plants. In previous studies, LRR1 was shown to suppress HIR1-triggered cell death as a negative regulator in *Arabidopsis* and tobacco (Jung and Hwang, 2007; Choi et al., 2011). In contrast with these previous findings, LRR1 physically interacts with PR10 and enhances PR10-triggered cell

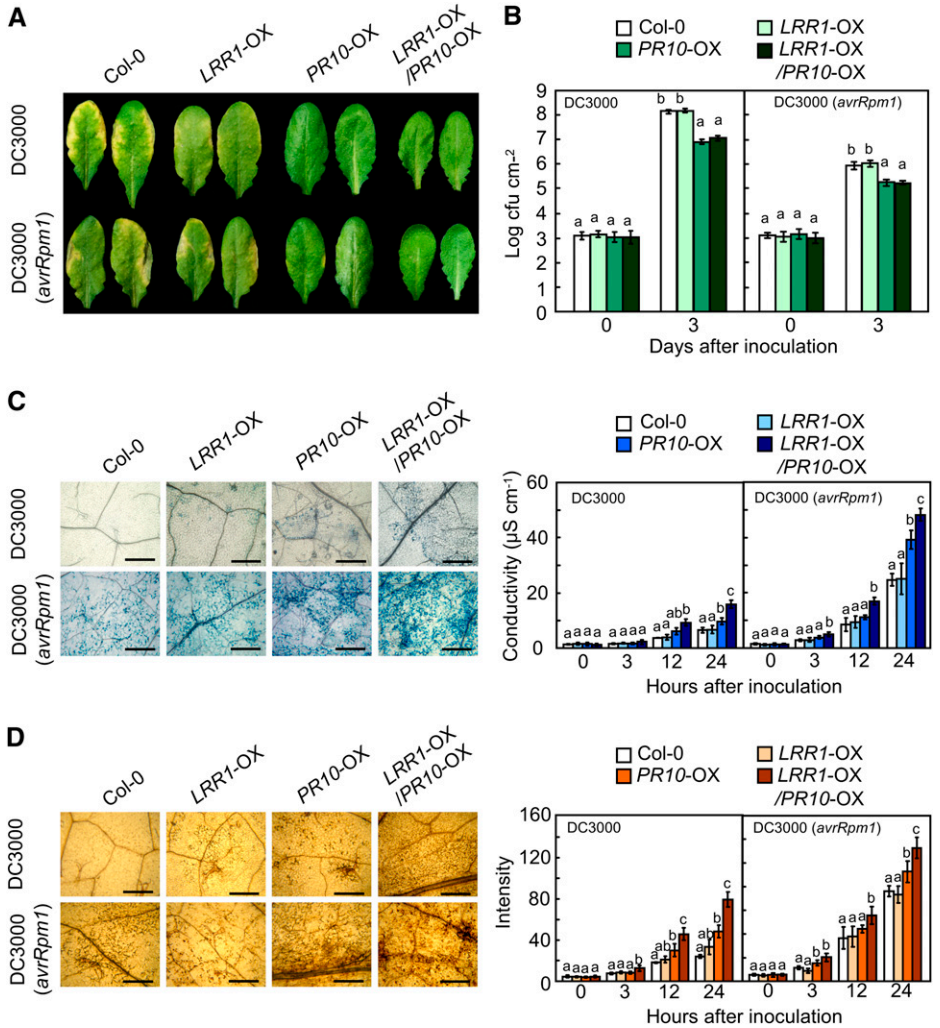

Figure 8. Enhanced Resistance of *PR10*- and *LRR1*/*PR10*-OX Transgenic *Arabidopsis* Plants to *Pst* Infection.

(A) Disease symptoms on leaves 72 h after inoculation.

(B) Bacterial growth in the leaves of wild-type and transgenic plants.

(C) Micrographs of the leaves stained with trypan blue (left) 24 h after infiltration and quantification of electrolyte leakage (right) from leaf discs. Bars = 500 μm.

(D) Micrographs of the leaves stained with DAB (left) 24 h after inoculation and intensity of the reddish color from DAB images (right) to assess H_2O_2 production. Bars = 500 μm.

(B) to **(D)** Data represent the means ± SD from three independent experiments. Different letters indicate significant differences, as statistically analyzed by Fisher's protected LSD test ($P < 0.05$).

death and defense responses as a positive regulator. Interestingly, the transient coexpression of *LRR1* with *PR10* intensifies *PR10*-triggered cell death, suggesting that the cell death induction by PR10 may require complex formation with LRR1. The conflicting evidence that LRR1 with HIR1 or PR10 acts as a negative or positive regulator, respectively, may reflect the distinct functions of both HIR1 and PR10 for disease-associated and HR-associated cell death, respectively. This suggestion is supported by the experimental finding that silencing of *HIR1* in pepper significantly compromised HR and disease-associated cell deaths (Choi et al., 2011). Unlike pepper, transient expression of *PR10* alone does not induce a typical cell death response in *N. benthamiana* leaves. Moreover, immunoblot detection of the transient expression indicated that neither PR10 nor LRR1 induces each other in pepper leaves (Figure 2A). These results suggest that PR10 requires specific pepper components for cell death induction. The Bet v I fold domain present in PR10 has been demonstrated to be responsible for its interaction with several ligands, such as brassinosteroids, cytokinin, and flavonoid (Fujimoto et al., 1998; Mogensen et al., 2002; Marković-Housley et al., 2003; Koistinen et al., 2005), suggesting that it might be involved in PR10 binding to LRR1. However, further studies using domain mutants will be required to elucidate the binding site of PR10 for LRR1.

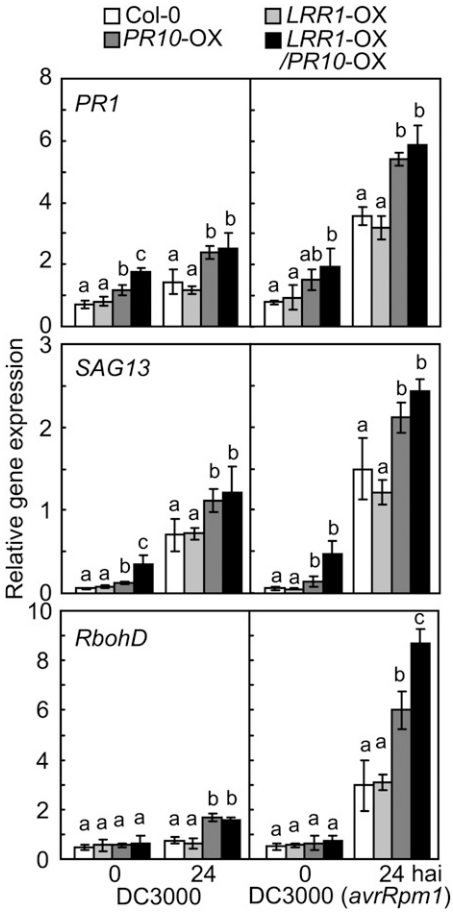

Figure 9. Real-Time RT-PCR Analysis of Defense Marker Gene Expression in *LRR1*-, *PR10*-, and *LRR1/PR10*-OX Transgenic *Arabidopsis* Plants.

Expression values are normalized by the expression level of *ACTIN2*. Data represent the means ± SD from three independent experiments. Different letters indicate significant differences, as analyzed by Fisher's protected LSD test ($P < 0.05$). hai, hours after inoculation with *Pst* DC3000.

LRR1 Promotes the Ribonuclease Activity and Phosphorylation of PR10

It has been reported that PR10 is phosphorylated (Ziadi et al., 2001) and that its phosphorylation is required for the defense response to microbial pathogen attack (Park et al., 2004). In this study, we also show that recombinant PR10 has RNase activity and that it is phosphorylated by crude protein extracts from pepper leaves infected by avirulent *Xcv* Bv5-4a. The plant protein extracts were used as an alternative kinase pool because there is no information about which kinase is involved in PR10 phosphorylation. Notably, LRR1 potentiates the RNase activity of PR10. RNase activity is thought to be essential for the resistance response to microbial pathogens (Barna et al., 1989; Lusso and Kuc, 1995; Galiana et al., 1997; Shivakumar et al., 2000; Park et al., 2004). In this study, LRR1 is also shown to be a potential stimulator of PR10 phosphorylation, which could lead to the activation of defense and HR-like cell death. Together, these results suggest that the phosphorylation and RNase activity of pepper PR10, which is increased by its interaction with LRR1, may be required for cell death and defense induction.

Cytoplasmic Localization of the LRR1-PR10 Complex Is Essential for the Induction of the Cell Death Response

BiFC analysis enables the direct visualization of protein–protein interactions to determine the subcellular site of interaction (Walter et al., 2004). YFP signals of the LRR1-PR10 complex were detected in the cytoplasmic region of *N. benthamiana* leaves at early time point after agroinfiltration but in both the cytoplasmic and apoplastic regions at late time point. This suggests the export of the LRR1-PR10 complex into the apoplastic space during the cell death response. The localization of the LRR1-PR10 complex in the apoplast region may not be responsible for cell death, but rather a consequence caused by cell wall degradation.

Certain plant disease resistance proteins act in specific subcellular locations to trigger downstream signaling and defense pathways. Some NB-LRR–type immune receptors enter and function in the nucleus (Sheen and He, 2007; Shen and Schulze-Lefert, 2007). Barley (*Hordeum vulgare*) mildew A 10 (Shen et al., 2007), *Arabidopsis* RPS4 (Wirthmueller et al., 2007), and tobacco N protein (Burch-Smith et al., 2007) are functional in the nucleus. By contrast, potato Rx1 activates an antiviral mechanism in the cytoplasm but not in the nucleus (Slootweg et al., 2010). The NB-LRR–type R protein, RECOGNITION OF PERONOSPORA PARASITICA1A, is targeted to the plasma membrane and associates with the endoplasmic reticulum and the Golgi apparatus (Michael Weaver et al., 2006). In this study, PR10 interacts with LRR1 in the cytoplasm to trigger defense signaling. The hypersensitive-induced reaction protein, HIR1, was demonstrated to physically interact with LRR1, which possesses four LRR domains for their association (Jung and Hwang, 2007). Interestingly, extracellular LRR1 interacts with membrane-associated HIR1 to form membrane microdomains (Choi et al., 2011). Since LRR1 has a putative signal peptide sequence in N terminus (Jung et al., 2004), this protein is predicted to be involved in the cellular secretion. Choi et al. (2011) showed that LRR1 was localized in small patches at the plasma membrane when it was expressed in onion (*Allium cepa*) epidermal cells and also that it was enriched in the extracellular protein extract from pepper leaves infected with *Xcv*. In our experiments, GFP-fused LRR1 under the 35S promoter was predominantly visualized in the cytoplasmic region along with the plasma membrane in epidermal cells of *N. benthamiana* leaves (Figure 5). Therefore, the relatively small LRR1 protein may flexibly interact with both cytosolic and membrane-anchored proteins during transport from the intracellular region to the apoplastic space.

We attempted to engineer the LRR1-PR10 interaction site to determine whether the cytoplasmic localization of the LRR1-PR10 complex is essential for the cell death induction. The attachment of an NLS (Hodel et al., 2001) recruited both LRR1 and PR10 into the nucleus, where they were able to form a protein–protein association (Figure 5B). However, nuclear pools of the LRR1 and PR10 complex were not able to trigger the HR

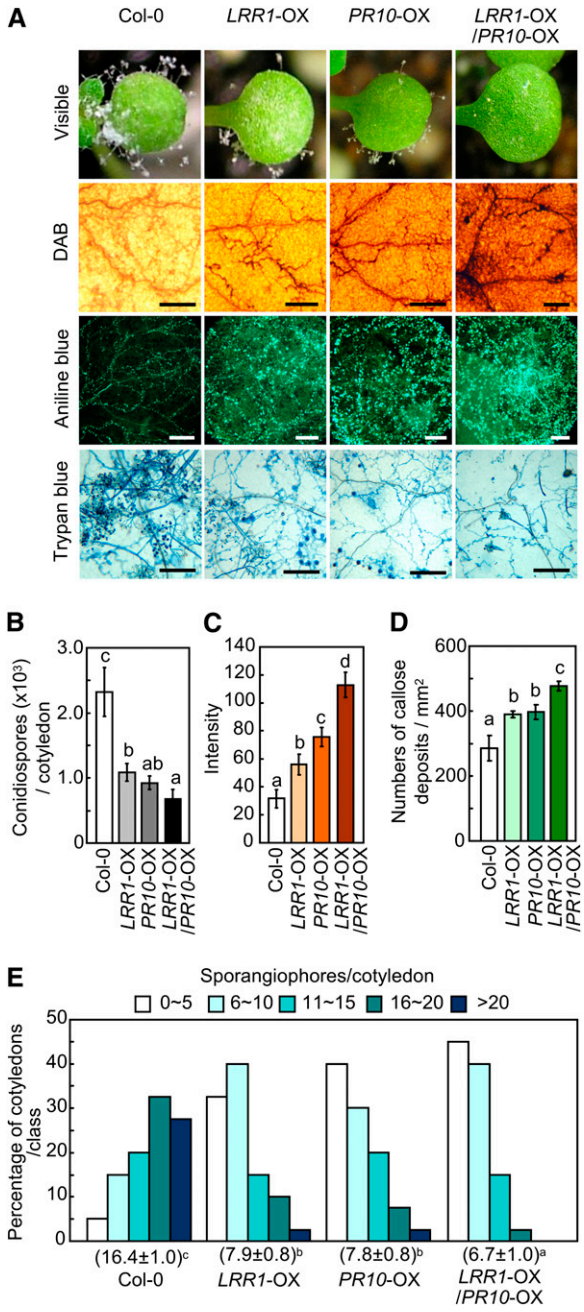

Figure 10. Enhanced Resistance of *LRR1*-, *PR10*-, and *LRR1/PR10*-OX Transgenic *Arabidopsis* Plants to *H. arabidopsidis* Infection.

(A) Disease symptoms and cell responses in the cotyledons inoculated with conidiospores of *H. arabidopsidis* isolate Noco2. Bars = 200 μm.
(B) Quantification of conidiospores on 20 cotyledons.
(C) ROS intensities of leaf tissues, as measured by a color densitometer using ImageJ software after DAB staining.
(D) Quantification of callose deposition by aniline blue staining.
(E) Quantification of asexual sporangiophores on cotyledons. The numbers below each line represent the means ± SD.
(B) to **(E)** Data represent the means ± SD from three independent experiments. Different letters indicate significant differences, as analyzed by Fisher's protected LSD test ($P < 0.05$).

phenotype. When fused with nls, the LRR1-PR10 complexes were sequestered in the cytoplasm. The coexpression of nls-LRR1 and nls-PR10 induced the hypersensitive cell death response in *N. benthamiana* leaves (Figure 5E). These results suggest a requirement for the downstream signaling of this complex in the cytoplasm.

LRR1 and PR10 Play a Role in Cell Death and Defense Responses in Pepper and *Arabidopsis*

PR10 proteins have been identified as essential for the primary detectable defense response of resistant and susceptible plants to biotic attack. The PR10 protein level is significantly higher in *Fusarium graminearum*–infected resistant maize (*Zea mays*) inbred CO441 than in *F. graminearum*–susceptible inbred B73 (Mohammadi et al., 2011). In our study, pepper *PR10* is rapidly and strongly induced at transcriptional and protein levels in the incompatible response during *Xcv* infection. This finding strongly supports a critical role of pepper PR10 in disease resistance. By contrast, silencing of PR10-like proteins in *Medicago truncatula* results in an antagonistic induction of other pathogenesis-related proteins and in an increased tolerance upon infection with the necrotrophic oomycete *Aphanomyces euteiches* (Colditz et al., 2007).

In this study, *PR10* silencing significantly compromises bacterial growth restriction, cell death response, and ROS accumulation in pepper leaves during infection with incompatible *Xcv* Bv5-4a. *LRR1* positively regulates the *PR10*-triggered cell death that is accompanied by increased ROS levels. To support these early defense events, the silencing of *PR10* or *LRR1/PR10* significantly compromised the induction of pepper defense marker genes, such as *PR1* (Kim and Hwang, 2000), *DEF1* (Do et al., 2004), *SAR82* (Lee and Hwang, 2003), and *PO2* (Choi et al., 2007), as well as the accumulation of SA, especially by avirulent *Xcv* infection. In general, the SA-dependent pathway positively regulates defense response against biotrophic pathogen infection (Spoel and Dong, 2008). These findings support the possibility that the LRR1-PR10 complex may regulate the cell death and defense response by affecting downstream defense genes and SA signaling pathways.

Overexpression of both *PR10* and *LRR1* suppressed *Pst* DC3000 growth at a level similar to that observed in the single *PR10*-OX plant. However, the enhanced cell death noted in the *PR10/LRR1* double mutant plants supports the potential ability of these genes to function in plant immunity against pathogen invasion. This enhanced cell death effect was also ascertained by a downy mildew infection assay. Co-overexpression of *PR10/LRR1* confers enhanced resistance to infection by *H. arabidopsidis* Noco2, and this resistance is accompanied by an increase in ROS and callose production around the infection sites. These findings suggest that the PR10 and LRR1 complex is effective in triggering the defense response to infection by the biotrophic oomycete.

Proposed Model for the Role of the PR10 and LRR1 Complex in Cell Death–Mediated Defense Signaling

Combining the data presented here, we propose a working model for the role of the PR10 and LRR1 complex in cell death–

mediating defense signaling in plants (see Supplemental Figure 9 online). During incompatible *Xcv* infection, PR10, along with the positive regulator LRR1, induces early defense responses, including callose accumulation, SA and ROS burst, and defense-related gene expression. In addition, LRR1 enhances the phosphorylation and RNase activity of PR10, which may be required for cell death and defense induction. These ultimately lead to HR-like cell death and the basal defense response. In a previous study, transient expression assays showed that LRR1 negatively regulates HIR1-mediated cell death associated with disease (Choi et al., 2011). It seems likely that HIR1 is primarily involved in disease-associated cell death, whereas PR10 may trigger HR cell death and defense. This suggests that LRR1 has a dual function in cell death regulation. There is convincing evidence to indicate that host-controlled PCD is intimately linked with the onset of disease-associated cell death and symptom development (Greenberg and Yao, 2004). During virulent *Xcv* infection, *Xcv* effectors suppress pathogen-associated molecular pattern–triggered immunity, where HIR1 signaling induces disease-associated cell death (Choi et al., 2011). It is not determined whether PR10 competes with HIR1 for the interaction with LRR1; however, *LRR1* induction may promote *PR10*-mediated hypersensitive cell death and resistance responses against avirulent *Xcv* infection. The LRR1-PR10 interaction also activates the cell death pathway in pepper, *N. benthamiana*, and *Arabidopsis*. LRR1 physically interacts with PR10 and acts as a positive regulator to enhance PR10-triggered cell death and defense signaling. However, how LRR1 activates PR10-dependent resistance remains to be clarified. More detailed studies of the molecular mechanisms underlying the disease resistance-associated specific interaction between PR10 and LRR1 are needed.

METHODS

Plant Materials and Pathogen Inoculation

Pepper (*Capsicum annuum* cv Nockwang) and *Nicotiana benthamiana* plants were raised in a growth room at 26°C with a 16-h-light/8-h-dark cycle. Fully expanded pepper leaves were infiltrated with *Xanthomonas campestris* pv *vesicatoria* strains Ds1 (virulent) and Bv5-4a (avirulent).

Arabidopsis thaliana (ecotype Col-0) plants were grown in soil under controlled environmental conditions (16-h-light/8-h-dark cycle, 24°C, and 100 μmol photons m^{-2} s^{-1}). *Pseudomonas syringae* pv *tomato* DC3000 and DC3000 (*avrRpm1*) were infiltrated into *Arabidopsis* leaves. *Hyaloperonospora arabidopsidis* isolate Noco2 was maintained on *Arabidopsis* (Col-0) seedlings. Ten-day-old *Arabidopsis* seedlings were spray-inoculated with a suspension of 5×10^4 conidiosporangia mL^{-1}. The disease rating was conducted as previously described (Lee et al., 2008).

RNA Gel Blot and Quantitative Real-Time RT-PCR Analyses

Total RNA was isolated using TRIzol reagent (Invitrogen), according to the manufacturer's instructions. RNA gel blot analysis was conducted following standard procedures. Total RNA was transferred to a nylon membrane and probed with ^{32}P-labeled LRR1 and PR10 open reading frames, which were generated from the plasmid by *Eco*RI digestion. RT reactions were performed using 1 μg total RNA, 500 ng oligo$(dT)_{18}$ primer, and Moloney Murine Leukemia Virus Reverse Transcriptase (Enzynomics) at 42°C for 1 h. RT reaction products were used for quantitative real-time RT-PCR analysis. To normalize the transcript levels, *β-tubulin* and *ACTIN2* expression was monitored in *N. benthamiana* and *Arabidopsis*, respectively. The gene-specific primer sets used for the quantitative real-time RT-PCR analysis are listed in Supplemental Table 1 online.

Yeast Two-Hybrid Assay

The GAL4 system was used for the yeast two-hybrid assay according to the manufacturer's instructions (Invitrogen). The *LRR1* and *PR10* coding regions were PCR amplified and cloned into pCR2.1-TOPO (Invitrogen) using the primers listed in Supplemental Table 2 online. The constructs were recombined into the pGADT7 and pGBKT7 destination vectors, including the GAL4 DNA activation domain (AD) and binding domain (BD), respectively, to create AD/PR10, BD/LRR1, AD/LRR1, and BD/PR10. All of the constructs were transformed into yeast strain AH109. The positive clones were selected by growing on SD/-Leu/-Trp medium, followed by growth on SD/-Leu/-Trp/-Ade/-His medium. The final clones were arrayed on SD/-Leu/-Trp/-Ade/-His medium containing 40 mg L^{-1} X-Gal and 20 g L^{-1} Gal.

BiFC Analysis

For the BiFC constructs, *LRR1* and *PR10* were PCR amplified using the primers listed in Supplemental Table 2 online. The fragments were cloned into pCR2.1/TOPO and then recombined into pSPYNE or pSPYCE, resulting in pSPYNE:*LRR1*, pSPYCE:*PR10*, or vice versa, as described (Walter et al., 2004). *Agrobacterium tumefaciens* strain GV3101 harboring the BiFC constructs was coinfiltrated into *N. benthamiana* leaves. One day after agroinfiltration, the leaves were visualized using an LSM 5 Exciter confocal laser scanning microscope (Carl Zeiss) with excitation at 514 nm and emission at 525 to 600 nm. When indicated, BFA (10 μg mL^{-1}) was infiltrated into *N. benthamiana* leaves 24 h after agroinfiltration of the BiFC or GFP constructs.

Co-IP

For co-IP constructs, *LRR1* and *PR10* were PCR amplified using the primers listed in Supplemental Table 2 online. The fragments were cloned into pCR2.1/TOPO and recombined into p35S:6HA or p35S:8Myc. *Agrobacterium* strain GV3101 harboring the constructs was coinfiltrated into *N. benthamiana* leaves. Proteins were extracted from leaf samples using extraction buffer (10% glycerol, 25 mM Tris-HCl, pH 7.5, 150 mM NaCl, 1 mM EDTA, 1% Triton X-100, 10 mM DTT, 1× complete protease inhibitor cocktail [Roche], and 2% [w/v] polyvinyl polypyrrolidone). The protein extracts were incubated with monoclonal anti-HA or anti-Myc agarose (Sigma-Aldrich) overnight. Beads were collected and washed with immunoprecipitation buffer (10% glycerol, 25 mM Tris-HCl, pH 7.5, 150 mM NaCl, 1 mM EDTA, 0.15% Nonidet P-40, and 2 mM DTT). Eluted proteins were analyzed by immunoblotting using monoclonal anti-HA-peroxidase antibody (Sigma-Aldrich) or polyclonal anti-c-Myc-peroxidase antibody (Sigma-Aldrich). Immunodetection was performed using the WESTZOL plus protein gel blot detection system (iNtRON Biotechnology).

Antibody Production and Immunoblot Analysis

The polyclonal rabbit antibodies were raised against recombinant PR10 (Young In Frontier). The full-length PR10 and LRR1 coding regions were PCR amplified from pepper cDNA using the primers listed in Supplemental Table 2 online. The fragments of PR10 and LRR1 were integrated into the *Bam*HI and *Sac*I sites of the pET28a expression vector (Invitrogen) expressing an N-terminal His-tag and into the pGEX-5X expression vector (GE Healthcare) expressing an N-terminal GST tag, respectively. His-PR10 and GST-LRR1 fusion proteins were expressed in *Escherichia coli* BL21, purified, and injected into rabbits. The rabbit antisera were purified using a column conjugated with protein A resin (Sigma-Aldrich).

Total proteins were extracted from the leaves, as described previously (Choi et al., 2008). For immunoblot analysis, equal amounts of protein

were separated by SDS-PAGE and blotted to polyvinylidene fluoride membranes. The membranes were probed with LRR1- and PR10-specific antibodies at 1:5000 and 1:10,000 dilution, respectively. Horseradish peroxidase–conjugated goat anti-rabbit IgG (Sigma-Aldrich) was used as a secondary antibody.

RNase Activity Assay

An in-gel RNase activity assay of recombinant PR10 and LRR1 was performed using the torula yeast (*Candida utiliz*) RNA (Sigma-Aldrich), as described (Yen and Green, 1991). Recombinant PR10 and LRR1 were purified from *E. coli* transformed with pET28a and pGEX-5X using Ni-NTA resin (Invitrogen) and Glutathione Sepharose 4B (GE Healthcare), respectively. The recombinant or control proteins were mixed with a protein loading dye and loaded onto 15% acrylamide gel containing 2.4 mg mL^{-1} of yeast RNA. The electrophoresis for protein separation was performed in a Mini PROTEAN 3 cell (Bio-Rad).

RNase activity was determined according to the method of Barna et al. (1989) with minor modifications. Yeast RNA (200 μg) mixed with PR10 and LRR1 (0.1 to ~5.0 μg) was incubated in 400 μL of 100 mM MES, pH 6.0, at 56°C for 30 min. One unit of RNase activity was defined as an increase in absorbance of 1.0 at OD_{260} after incubation for 30 min.

Phosphorylation Assay

Phosphorylation assay was performed as described by Park et al. (2004), with minor modifications. The pepper leaves inoculated with avirulent *Xcv* strain Bv5-4a (10^8 cfu mL^{-1}) were homogenized in extraction buffer (40 mM Tris-HCl, pH 7.8, 1 mM DTT, 10% glycerol, 0.2 mM sodium fluoride, 0.1 mM sodium pyrophosphate, and 1× protease inhibitor cocktail). The phosphorylation reaction was done at 30°C for 20 min after addition of recombinant PR10 and LRR into the buffer (20 μg proteins in the leaf extract, 5 mM $MgCl_2$, 100 μM ATP, and 25 mM KCl). His or GST fusion protein purification was performed using the standard protocol of Ni-NTA purification (Invitrogen) and a GST fusion protein purification system (GE Healthcare), respectively. His or GST fusion protein was immunoprecipitated using a His or GST antibody (Sigma-Aldrich). Immunodetection was performed using anti-His (Santa Cruz), anti-GST (Santa Cruz), and anti-phosphoserine (Sigma-Aldrich) at 1:10,000 dilution.

For detection of phosphoprotein, Pro-Q diamond phosphoprotein staining (Martin et al., 2003; Wang et al., 2005) was used as described by the manufacturer (Invitrogen). After one-dimensional electrophoresis, the gel was stained with Pro-Q diamond in the dark for 60 min and then destained with 100 mL of 20% acetonitrile and 50 mM sodium acetate, pH 4.0. Gel image capture and phosphoprotein quantification were performed using ProXPRESS (Perkin-Elmer LifeScience) with 540/25-nm excitation and 590/30-nm emission filters.

Agrobacterium-Mediated Transient Expression and Subcellular Localization Assays

For the generation of pBIN35S-GFP constructs, *LRR1* and *PR10* were PCR amplified using the primers listed in Supplemental Table 2 online. The fragments were cloned into pCR2.1/TOPO and recombined into pBIN35S-GFP. *Agrobacterium* strain GV3101 carrying the constructs was grown overnight in Luria-Bertani liquid medium containing 50 μg mL^{-1} kanamycin and 50 μg mL^{-1} rifampicin. Bacterial cells were infiltrated into pepper or *N. benthamiana* leaves. For comparison, *Bax* and *avrPto*/*Pto* was transiently expressed in *N. benthamiana* leaves (Choi et al., 2011).

GFP was visualized using a LSM 5 Exciter confocal laser scanning microscope (Carl-Zeiss) with excitation at 48 8 nm and emission at 505 to 530 nm. For visualization of the nuclei, detached leaves were immersed in staining buffer (0.1% 4′,6-diamidino-2-phenylindole [DAPI] in 5% DMSO). The DAPI fluorescence images were obtained using excitation at 405 nm and emission at 435 to 480 nm.

Engineering of Nuclear Expression

For nuclear localization, the NLS was fused to the N terminus of *LRR1* or *PR10*. The nls sequence contains a Lys residue substituted with an Asn residue. The nls, which fails to target to the nuclei, was included as a negative control. The sequences used were NLS (5′-GGCCCTAAAAAGAAGCG-TAAGGTT-3′) and nls (5′- GGCCCTAAAAACAAGCGTAAGGTT-3′) (Hodel et al., 2001).

Nuclear fractionation was conducted as previously described (Tameling et al., 2010). Leaf tissues were homogenized in Honda buffer (2.5% Ficoll 400, 5% dextran T40, 0.4 M Suc, 25 mM Tris-HCl, pH 7.5, 10 mM $MgCl_2$, 1 mM DTT, 1 mM phenylmethanesulfonylfluoride, and a complete protease inhibitor cocktail). Triton X-100 was added to a final concentration of 0.5%. The harvested supernatant represented the soluble fraction, and the pellet was purified as a nuclear fraction. The two phase fractions were subjected to immunoblot analysis. Anti-H3 (Abcam) and anti-heat shock complex 70 (Abcam) were used as nuclear and cytosolic protein markers, respectively.

VIGS

To investigate the loss of function of LRR1 and PR10, tobacco rattle virus (TRV)-based VIGS assays were performed as described previously (Liu et al., 2002; Hwang et al., 2011). *LRR1*- and *PR10*-specific 5′-untranslated region was PCR amplified and cloned into the pTRV2 vector using the primer sets listed in Supplemental Table 2 online. *Agrobacterium* GV3101 carrying TRV-derived plasmids (TRV1, TRV2-*LRR1*, and TRV2-*PR10*) were cultured in Luria-Bertani liquid medium containing 50 μg mL^{-1} kanamycin and 50 μg mL^{-1} rifampicin. The cultures were centrifuged and resuspended in infiltration medium (10 mM MES, pH 5.6, 10 mM $MgCl_2$, and 200 μM acetosyringone). *Agrobacterium* suspensions containing TRV1 or TRV2 constructs were mixed at a 1:1 ratio and coinfiltrated into the cotyledons of 2-week-old pepper seedlings.

Arabidopsis Transformation

The *PR10* coding region was PCR amplified using specific primer sets (see Supplemental Table 2 online) and cloned into the *Xba*I and *Bam*HI sites of the binary vector pBIN35S (Choi and Hwang, 2011). The resulting binary plasmid was transformed into *Agrobacterium* strain GV3101 by electroporation. The *Agrobacterium*-mediated transformation was performed using the floral dipping method (Clough and Bent, 1998). Transgenic plants were selected by germinating seeds on Murashige and Skoog agar medium containing 50 μg mL^{-1} kanamycin. *LRR1*-OX *Arabidopsis* seeds were obtained from the laboratory seed stocks (Jung and Hwang, 2007). Transgenic *Arabidopsis* plants overexpressing both *LRR1* and *PR10* were generated by crossing the two OX mutant lines.

Measurement of Ion Conductivity

Ion leakage was measured as previously described (Hwang and Hwang, 2011; Lee et al., 2011). The leaf discs (8 mm in diameter) were washed and incubated in 10 mL of double distilled water for 30 min at room temperature. The ion conductivity was recorded using a sensION7 conductivity meter (Hach).

SA Quantification

SA and its glucoside (SAG) were extracted from pepper leaves and analyzed using HPLC, as described previously (Choi and Hwang, 2011; Kim and Hwang, 2011). HPLC separation was achieved using a 5-μm Xbridge C18 reverse-phase column (4.6 mm × 250 mm; Waters) fitted with an Xbridge C18 guard column (5 mm × 4.6320 mm; Waters). SA levels were measured using

a fluorescence detector (Photo Diode Array Detector; Waters) with excitation at 305 nm and emission at 405 nm. 3-Hydroxybenzoic acid (Sigma-Aldrich) was included as an internal standard.

Histochemical Assay

DAB was used to stain H_2O_2-producing leaves. The leaves were incubated in 1% DAB solution in the dark overnight and destained with lactic acid/glycerol/ethanol (1:1:2). ImageJ software (National Institutes of Health) was used for quantification of H_2O_2 accumulation from the DAB images. To visualize the cell death response, the infiltrated leaves were stained with trypan blue and destained with saturated chloral hydrate solution (2.5 g mL^{-1}). Epifluorescence microscopy was used to detect callose deposits after staining with aniline blue. Infiltrated leaves were cleared in alcoholic lactophenol (95% ethanol:lactophenol = 2:1; lactophenol, phenol:glycerol:lactic acid:water = 1:1:1:1). Cleared leaves were stained with 0.01% aniline blue in 0.15 M phosphate buffer, pH 9.5. Callose deposition was visualized with a fluorescence microscope under UV light.

Accession Numbers

Sequence data from this article can be found in the GenBank/EMBL data libraries under the following accession numbers: pepper *LRR1* (AY237117), pepper *PR10* (AF244121), pepper *PR1* (AF053343), pepper *DEF1* (AF442388), pepper *SAR82A* (AF313766), pepper *PO2* (DQ489711), pepper *ACT* (GQ339766), *N. benthamiana VPE1a* (AB075947), *N. benthamiana HSR203J* (AB091430), *N. benthamiana β-TUB2* (U91563), *Arabidopsis PR1* (AT2G14610), *Arabidopsis SAG13* (AT2G29350), *Arabidopsis RbohD* (AT5G47910), and *Arabidopsis ACT2* (AT3G18780).

Supplemental Data

The following materials are available in the online version of this article.

Supplemental Figure 1. Expression Patterns of *PR10* in Pepper Leaves Infected with *Xcv*.

Supplemental Figure 2. LRR1 and PR10 Interact in the Cytoplasm and Are Released into the Apoplast.

Supplemental Figure 3. Localization of the LRR1 and PR10 Complex in *N. benthamiana* Leaves Treated with BFA.

Supplemental Figure 4. Quantitative Real-Time RT-PCR Analysis of the Expression of *LRR1* and/or *PR10* in VIGS Pepper Leaves Infected with *Xcv*.

Supplemental Figure 5. Enhanced Resistance of *PR10*-OX *Arabidopsis* Lines to *Pst* Infection.

Supplemental Figure 6. PR10 Contributes to Basal Resistance by Callose Deposition.

Supplemental Figure 7. Transgenic *Arabidopsis* Plants Overexpressing *LRR1* and/or *PR10.*

Supplemental Figure 8. Enhanced Resistance of *PR10*-OX *Arabidopsis* Lines to *Hpa* Infection.

Supplemental Figure 9. Proposed Model for the Role of the PR10 and LRR1 Complex in Cell Death–Mediating Defense Signaling in Plants.

Supplemental Table 1. Gene-Specific Primers for qRT-PCR Used in This Study.

Supplemental Table 2. Primers for Generation of Various Gene Constructs Used in This Study.

Supplemental Data Set 1. Text File of Details of Growth Phenotypes and Enhanced Disease Resistance of *PR10* Transgenic *Arabidopsis* Shown in Supplemental Figures 5 to 8.

ACKNOWLEDGMENTS

This work was supported by the Next Generation BioGreen21 Program (Plant Molecular Breeding Center; No. PJ008027), Rural Development Administration, Republic of Korea.

AUTHOR CONTRIBUTIONS

D.S.C. and B.K.H. designed the research and wrote the article. D.S.C. and I.S.H. performed the experiments and analyzed the data.

Received January 29, 2012; revised March 16, 2012; accepted March 21, 2012, published April 6, 2012.

REFERENCES

Barna, B., Ibenthal, W.D., and Heitefuss, R. (1989). Extracellular RNase activity in healthy and rust-infected wheat leaves. Physiol. Mol. Plant Pathol. **35:** 151–160.

Breiteneder, H., Pettenburger, K., Bito, A., Valenta, R., Kraft, D., Rumpold, H., Scheiner, O., and Breitenbach, M. (1989). The gene coding for the major birch pollen allergen *Betv1*, is highly homologous to a pea disease resistance response gene. EMBO J. **8:** 1935–1938.

Brodersen, P., Petersen, M., Pike, H.M., Olszak, B., Skov, S., Ødum, N., Jørgensen, L.B., Brown, R.E., and Mundy, J. (2002). Knockout of *Arabidopsis ACCELERATED-CELL-DEATH11* encoding a sphingosine transfer protein causes activation of programmed cell death and defense. Genes Dev. **16:** 490–502.

Bufe, A., Spangfort, M.D., Kahlert, H., Schlaak, M., and Becker, W.-M. (1996). The major birch pollen allergen, *Bet v 1*, shows ribonuclease activity. Planta **199:** 413–415.

Burch-Smith, T.M., Schiff, M., Caplan, J.L., Tsao, J., Czymmek, K., and Dinesh-Kumar, S.P. (2007). A novel role for the TIR domain in association with pathogen-derived elicitors. PLoS Biol. **5:** e68.

Choi, D.S., and Hwang, B.K. (2011). Proteomics and functional analyses of pepper *abscisic acid-responsive 1* (*ABR1*), which is involved in cell death and defense signaling. Plant Cell **23:** 823–842.

Choi, H.W., Lee, B.G., Kim, N.H., Park, Y., Lim, C.W., Song, H.K., and Hwang, B.K. (2008). A role for a menthone reductase in resistance against microbial pathogens in plants. Plant Physiol. **148:** 383–401.

Choi, H.W., Kim, Y.J., and Hwang, B.K. (2011). The hypersensitive induced reaction and leucine-rich repeat proteins regulate plant cell death associated with disease and plant immunity. Mol. Plant Microbe Interact. **24:** 68–78.

Choi, H.W., Kim, Y.J., Lee, S.C., Hong, J.K., and Hwang, B.K. (2007). Hydrogen peroxide generation by the pepper extracellular peroxidase CaPO2 activates local and systemic cell death and defense response to bacterial pathogens. Plant Physiol. **145:** 890–904.

Clough, S.J., and Bent, A.F. (1998). Floral dip: A simplified method for *Agrobacterium*-mediated transformation of *Arabidopsis thaliana*. Plant J. **16:** 735–743.

Colditz, F., Niehaus, K., and Krajinski, F. (2007). Silencing of PR-10-like proteins in *Medicago truncatula* results in an antagonistic induction of other PR proteins and in an increased tolerance upon infection with the oomycete *Aphanomyces euteiches*. Planta **226:** 57–71.

Dangl, J.L., Dietrich, R.A., and Richberg, M.H. (1996). Death don't have no mercy: Cell death programs in plant-microbe interactions. Plant Cell **8:** 1793–1807.

Dangl, J.L., and Jones, J.D.G. (2001). Plant pathogens and integrated defence responses to infection. Nature **411:** 826–833.

Do, H.M., Lee, S.C., Jung, H.W., Sohn, K.H., and Hwang, B.K. (2004). Differential expression and in situ localization of a pepper defensin

(*CADEF1*) gene in response to pathogen infection, abiotic elicitors and environmental stresses in *Capsicum annuum*. Plant Sci. **166:** 1297–1305.

Fujimoto, Y., Nagata, R., Fukasawa, H., Yano, K., Azuma, M., Iida, A., Sugimoto, S., Shudo, K., and Hashimoto, Y. (1998). Purification and cDNA cloning of cytokinin-specific binding protein from mung bean (*Vigna radiata*). Eur. J. Biochem. **258:** 794–802.

Galiana, E., Bonnet, P., Conrod, S., Keller, H., Panabières, F., Ponchet, M., Poupet, A., and Ricci, P. (1997). RNase activity prevents the growth of a fungal pathogen in tobacco leaves and increases upon induction of systemic acquired resistance with elicitin. Plant Physiol. **115:** 1557–1567.

Gao, Z., Chung, E.-H., Eitas, T.K., and Dangl, J.L. (2011). Plant intracellular innate immune receptor Resistance to *Pseudomonas syringae pv. maculicola 1* (RPM1) is activated at, and functions on, the plasma membrane. Proc. Natl. Acad. Sci. USA **108:** 7619–7624. Erratum. Proc. Natl. Acad. Sci. USA **108:** 8915.

Gassmann, W., Hinsch, M.E., and Staskawicz, B.J. (1999). The *Arabidopsis RPS4* bacterial-resistance gene is a member of the TIR-NBS-LRR family of disease-resistance genes. Plant J. **20:** 265–277.

Gómez-Gómez, L., and Boller, T. (2000). FLS2: An LRR receptor-like kinase involved in the perception of the bacterial elicitor flagelin in *Arabidopsis.* Mol. Cell **5:** 1003–1011.

Greenberg, J.T., and Yao, N. (2004). The role and regulation of programmed cell death in plant-pathogen interactions. Cell. Microbiol. **6:** 201–211.

Gutierrez, J.R., Balmuth, A.L., Ntoukakis, V., Mucyn, T.S., Gimenez-Ibanez, S., Jones, A.M.E., and Rathjen, J.P. (2010). Prf immune complexes of tomato are oligomeric and contain multiple Pto-like kinases that diversify effector recognition. Plant J. **61:** 507–518.

Hashimoto, M., Kisseleva, L., Sawa, S., Furukawa, T., Komatsu, S., and Koshiba, T. (2004). A novel rice PR10 protein, RSOsPR10, specifically induced in roots by biotic and abiotic stresses, possibly via the jasmonic acid signaling pathway. Plant Cell Physiol. **45:** 550–559.

Hodel, M.R., Corbett, A.H., and Hodel, A.E. (2001). Dissection of a nuclear localization signal. J. Biol. Chem. **276:** 1317–1325.

Hwang, I.S., An, S.H., and Hwang, B.K. (2011). Pepper asparagine synthetase 1 (CaAS1) is required for plant nitrogen assimilation and defense responses to microbial pathogens. Plant J. **67:** 749–762.

Hwang, I.S., and Hwang, B.K. (2011). The pepper mannose-binding lectin gene *CaMBL1* is required to regulate cell death and defense responses to microbial pathogens. Plant Physiol. **155:** 447–463.

Jung, E.H., Jung, H.W., Lee, S.C., Han, S.W., Heu, S., and Hwang, B.K. (2004). Identification of a novel pathogen-induced gene encoding a leucine-rich repeat (LRR) protein expressed in phloem cells of *Capsicum annuum.* Biochim. Biophys. Acta **1676:** 211–222.

Jung, H.W., and Hwang, B.K. (2007). The leucine-rich repeat (LRR) protein, CaLRR1, interacts with the hypersensitive induced reaction (HIR) protein, CaHIR1, and suppresses cell death induced by the CaHIR1 protein. Mol. Plant Pathol. **8:** 503–514.

Jung, Y.-H., Lee, J.-H., Agrawal, G.K., Rakwal, R., Kim, J.-A., Shim, J.-K., Lee, S.-K., Jeon, J.-S., Koh, H.-J., Lee, Y.-H., Iwahashi, H., and Jwa, N.-S. (2005). The rice (*Oryza sativa*) *b*last *l*esion *m*imic mutant, *blm*, may confer resistance to blast pathogens by triggering multiple defense-associated signaling pathways. Plant Physiol. Biochem. **43:** 397–406.

Jung, Y.H., et al. (2006). Differential expression of defense/stress-related marker proteins in leaves of a unique rice blast lesion mimic mutant (*blm*). J. Proteome Res. **5:** 2586–2598.

Kim, D.S., and Hwang, B.K. (2011). The pepper receptor-like cytoplasmic protein kinase CaPIK1 is involved in plant signaling of defense and cell-death responses. Plant J. **66:** 642–655.

Kim, Y.J., and Hwang, B.K. (2000). Pepper gene encoding a basic pathogenesis-related 1 protein is pathogen and ethylene inducible. Physiol. Plant. **108:** 51–60.

Koistinen, K.M., Soininen, P., Venäläinen, T.A., Häyrinen, J., Laatikainen, R., Peräkylä, M., Tervahauta, A.I., and Kärenlampi, S.O. (2005). Birch PR-10c interacts with several biologically important ligands. Phytochemistry **66:** 2524–2533.

Lacomme, C., and Santa Cruz, S. (1999). Bax-induced cell death in tobacco is similar to the hypersensitive response. Proc. Natl. Acad. Sci. USA **96:** 7956–7961.

Lee, D.H., Choi, H.W., and Hwang, B.K. (2011). The pepper E3 ubiquitin ligase RING1 gene, *CaRING1*, is required for cell death and the salicylic acid-dependent defense response. Plant Physiol. **156:** 2011–2025.

Lee, S.C., and Hwang, B.K. (2003). Identification of the pepper SAR8.2 gene as a molecular marker for pathogen infection, abiotic elicitors and environmental stresses in *Capsicum annuum*. Planta **216:** 387–396.

Lee, S.C., Hwang, I.S., Choi, H.W., and Hwang, B.K. (2008). Involvement of the pepper antimicrobial protein *CaAMP1* gene in broad spectrum disease resistance. Plant Physiol. **148:** 1004–1020.

Li, Y., Tessaro, M.J., Li, X., and Zhang, Y. (2010). Regulation of the expression of plant resistance gene *SNC1* by a protein with a conserved BAT2 domain. Plant Physiol. **153:** 1425–1434.

Lim, J.H., Park, C.-J., Huh, S.U., Choi, L.M., Lee, G.J., Kim, Y.J., and Paek, K.-H. (2011). *Capsicum annuum* WRKYb transcription factor that binds to the CaPR-10 promoter functions as a positive regulator in innate immunity upon TMV infection. Biochem. Biophys. Res. Commun. **411:** 613–619.

Liu, J.J., and Ekramoddoullah, A.K.M. (2006). The family 10 of plant pathogenesis-related proteins: Their structure, regulation, and function in response to biotic and abiotic stresses. Physiol. Mol. Plant Pathol. **68:** 3–13.

Liu, Y.L., Schiff, M., and Dinesh-Kumar, S.P. (2002). Virus-induced gene silencing in tomato. Plant J. **31:** 777–786.

Lo, S.-C.C., Hipskind, J.D., and Nicholson, R.L. (1999). cDNA cloning of a sorghum pathogenesis-related protein (PR-10) and differential expression of defense-related genes following inoculation with *Cochliobolus heterostrophus* or *Colletotrichum sublineolum*. Mol. Plant Microbe Interact. **12:** 479–489.

Lorrain, S., Vailleau, F., Balagué, C., and Roby, D. (2003). Lesion mimic mutants: keys for deciphering cell death and defense pathways in plants? Trends Plant Sci. **8:** 263–271.

Lusso, M., and Kuc, J. (1995). Increased activities of ribonuclease and protease after challenge in tobacco plants with induced systemic resistance. Physiol. Mol. Plant Pathol. **47:** 419–428.

Marković-Housley, Z., Degano, M., Lamba, D., von Roepenack-Lahaye, E., Clemens, S., Susani, M., Ferreira, F., Scheiner, O., and Breiteneder, H. (2003). Crystal structure of a hypoallergenic isoform of the major birch pollen allergen Bet v 1 and its likely biological function as a plant steroid carrier. J. Mol. Biol. **325:** 123–133.

Martin, K., Steinberg, T.H., Cooley, L.A., Gee, K.R., Beechem, J.M., and Patton, W.F. (2003). Quantitative analysis of protein phosphorylation status and protein kinase activity on microarrays using a novel fluorescent phosphorylation sensor dye. Proteomics **3:** 1244–1255.

Matton, D.P., and Brisson, N. (1989). Cloning, expression, and sequence conservation of pathogenesis-related gene transcripts of potato. Mol. Plant Microbe Interact. **2:** 325–331.

McGee, J.D., Hamer, J.E., and Hodges, T.K. (2001). Characterization of a *PR-10* pathogenesis-related gene family induced in rice during infection with *Magnaporthe grisea*. Mol. Plant Microbe Interact. **14:** 877–886.

Melech-Bonfil, S., and Sessa, G. (2010). Tomato MAPKKKε is a positive regulator of cell-death signaling networks associated with plant immunity. Plant J. **64:** 379–391.

Michael Weaver, L., Swiderski, M.R., Li, Y., and Jones, J.D.G. (2006). The *Arabidopsis thaliana* TIR-NB-LRR R-protein, RPP1A; protein localization and constitutive activation of defence by truncated alleles in tobacco and Arabidopsis. Plant J. **47:** 829–840.

Moffett, P., Farnham, G., Peart, J., and Baulcombe, D.C. (2002). Interaction between domains of a plant NBS-LRR protein in disease resistance-related cell death. EMBO J. **21:** 4511–4519.

Mogensen, J.E., Wimmer, R., Larsen, J.N., Spangfort, M.D., and Otzen, D.E. (2002). The major birch allergen, Bet v 1, shows affinity for a broad spectrum of physiological ligands. J. Biol. Chem. **277:** 23684–23692.

Mohammadi, M., Anoop, V., Gleddie, S., and Harris, L.J. (2011). Proteomic profiling of two maize inbreds during early gibberella ear rot infection. Proteomics **11:** 3675–3684.

Mosher, S., Moeder, W., Nishimura, N., Jikumaru, Y., Joo, S.H., Urquhart, W., Klessig, D.F., Kim, S.K., Nambara, E., and Yoshioka, K. (2010). The lesion-mimic mutant *cpr22* shows alterations in abscisic acid signaling and abscisic acid insensitivity in a salicylic acid-dependent manner. Plant Physiol. **152:** 1901–1913.

Park, C.J., Kim, K.J., Shin, R., Park, J.M., Shin, Y.C., and Paek, K.H. (2004). Pathogenesis-related protein 10 isolated from hot pepper functions as a ribonuclease in an antiviral pathway. Plant J. **37:** 186–198.

Pontier, D., Godiard, L., Marco, Y., and Roby, D. (1994). hsr203J, a tobacco gene whose activation is rapid, highly localized and specific for incompatible plant/pathogen interactions. Plant J. **5:** 507–521.

Pühringer, H., Moll, D., Hoffmann-Spmmergruber, K., Watillon, B., Katinger, H., and Laimer da Camara Machado, M. (2000). The promoter of apple *Ypr 10* gene, encoding the major allerhen Mal d 1, is stress- and pathogen-inducible. Plant Sci. **152:** 35–50.

Sheen, J., and He, P. (2007). Nuclear actions in innate immune signaling. Cell **128:** 821–823.

Shen, Q.-H., Saijo, Y., Mauch, S., Biskup, C., Bieri, S., Keller, B., Seki, H., Ülker, B., Somssich, I.E., and Schulze-Lefert, P. (2007). Nuclear activity of MLA immune receptors links isolate-specific and basal disease-resistance responses. Science **315:** 1098–1103.

Shen, Q.-H., and Schulze-Lefert, P. (2007). Rumble in the nuclear jungle: Compartmentalization, trafficking, and nuclear action of plant immune receptors. EMBO J. **26:** 4293–4301.

Shivakumar, P.D., Vasanthi, N.S., Shetty, H.S., and Smedegaard-Petersen, V. (2000). Ribonucleases in the seedlings of pearl millet and their involvement in resistance against downy mildew disease. Eur. J. Plant Pathol. **106:** 825–836.

Slootweg, E., et al. (2010). Nucleocytoplasmic distribution is required for activation of resistance by the potato NB-LRR receptor Rx1 and is balanced by its functional domains. Plant Cell **22:** 4195–4215.

Somssich, I.E., Schmelzer, E., Bollmann, J., and Hahlbrock, K. (1986). Rapid activation by fungal elicitor of genes encoding "pathogenesis-related" proteins in cultured parsley cells. Proc. Natl. Acad. Sci. USA **83:** 2427–2430.

Spoel, S.H., and Dong, X. (2008). Making sense of hormone crosstalk during plant immune responses. Cell Host Microbe **3:** 348–351.

Staehelin, L.A., and Driouich, A. (1997). Brefeldin A effects in plants (Are different Golgi responses caused by different sites of action?). Plant Physiol. **114:** 401–403.

Tameling, W.I.L., Nooijen, C., Ludwig, N., Boter, M., Slootweg, E., Goverse, A., Shirasu, K., and Joosten, M.H.A.J. (2010). RanGAP2 mediates nucleocytoplasmic partitioning of the NB-LRR immune receptor Rx in the Solanaceae, thereby dictating Rx function. Plant Cell **22:** 4176–4194.

Tang, X., Frederick, R.D., Zhou, J., Halterman, D.A., Jia, Y., and Martin, G.B. (1996). Initiation of plant disease resistance by physical interaction of AvrPto and Pto kinase. Science **274:** 2060–2063.

Walter, M.H., Liu, J.W., Grand, C., Lamb, C.J., and Hess, D. (1990). Bean pathogenesis-related (PR) proteins deduced from elicitor-induced transcripts are members of a ubiquitous new class of conserved PR proteins including pollen allergens. Mol. Gen. Genet. **222:** 353–360.

Walter, M., Chaban, C., Schütze, K., Batistic, O., Weckermann, K., Näke, C., Blazevic, D., Grefen, C., Schumacher, K., Oecking, C., Harter, K., and Kudla, J. (2004). Visualization of protein interactions in living plant cells using bimolecular fluorescence complementation. Plant J. **40:** 428–438.

Wang, X., Goshe, M.B., Soderblom, E.J., Phinney, B.S., Kuchar, J.A., Li, J., Asami, T., Yoshida, S., Huber, S.C., and Clouse, S.D. (2005). Identification and functional analysis of in vivo phosphorylation sites of the *Arabidopsis* BRASSINOSTEROID-INSENSITIVE1 receptor kinase. Plant Cell **17:** 1685–1703.

Wang, Z.Y., Seto, H., Fujioka, S., Yoshida, S., and Chory, J. (2001). BRI1 is a critical component of a plasma-membrane receptor for plant steroids. Nature **410:** 380–383.

Warner, S.A.J., Scott, R., and Draper, J. (1992). Characterisation of a wound-induced transcript from the monocot asparagus that shares similarity with a class of intracellular pathogenesis-related (PR) proteins. Plant Mol. Biol. **19:** 555–561.

Wirthmueller, L., Zhang, Y., Jones, J.D.G., and Parker, J.E. (2007). Nuclear accumulation of the *Arabidopsis* immune receptor RPS4 is necessary for triggering EDS1-dependent defense. Curr. Biol. **17:** 2023–2029.

Yen, Y., and Green, P.J. (1991). Identification and properties of the major ribonucleases of *Arabidopsis thaliana*. Plant Physiol. **97:** 1487–1493.

Zhang, H., Dong, S., Wang, M., Wang, W., Song, W., Dou, X., Zheng, X., and Zhang, Z. (2010). The role of *vacuolar processing enzyme* (*VPE*) from *Nicotiana benthamiana* in the elicitor-triggered hypersensitive response and stomatal closure. J. Exp. Bot. **61:** 3799–3812.

Zhou, X.-J., Lu, S., Xu, Y.-H., Wang, J.-W., and Chen, X.-Y. (2002). A cotton cDNA (*GaPR-10*) encoding a pathogenesis-related 10 protein with in vitro ribonuclease activity. Plant Sci. **162:** 629–636.

Ziadi, S., Poupard, P., Brisset, M.-n., Paulin, J.P., and Simoneau, P. (2001). Characterization in apple leaves of two subclasses of PR-10 transcripts inducible by acibenzolar-S-methyl, a functional analogue of salicylic acid. Physiol. Mol. Plant Pathol. **59:** 33–43.

Zipfel, C., Kunze, G., Chinchilla, D., Caniard, A., Jones, J.D., Boller, T., and Felix, G. (2006). Perception of the bacterial PAMP EF-Tu by the receptor EFR restricts *Agrobacterium*-mediated transformation. Cell **125:** 749–760.